Iron and vitamin interactions in marine diatom isolates and natural assemblages of the Northeast Pacific Ocean

Natalie R. Cohen,[1] **Kelsey A. Ellis**,[1] **Wilton G. Burns**,[1] **Robert H. Lampe**,[1] **Nina Schuback**,[2] **Zackary Johnson**,[3] **Sergio Sañudo-Wilhelmy**,[4] **Adrian Marchetti**[1]*

[1]Department of Marine Sciences, University of North Carolina at Chapel Hill, Chapel Hill, North Carolina
[2]Department of Earth, Ocean, and Atmospheric Sciences, University of British Columbia, Vancouver, British Columbia, Canada
[3]Marine Laboratory, Nicholas School of the Environment and Biology Department, Duke University, Beaufort, North Carolina
[4]Department of Earth Sciences, University of Southern California, Los Angeles, California

Abstract

Trace metals and B-vitamins play critical roles in regulating marine phytoplankton growth and composition. While some microorganisms are capable of producing certain B-vitamins, others cannot synthesize them and depend on an exogenous supply. Therefore, external factors influencing vitamin synthesis, such as micronutrient concentrations, alter the extent to which B-vitamins are available to auxotrophs in surface waters. We examined iron, B_7 (biotin) and B_{12} (cobalamin) dynamics in diatoms through laboratory culture experiments and within natural diatom assemblages present along an iron gradient in the Northeast Pacific Ocean. In laboratory cultures of the diatom *Pseudo-nitzschia granii*, biotin synthase *(BIOB*) expression decreased 2-fold under iron limitation, suggesting iron status may affect B_7 production in diatoms. Additionally in laboratory cultures of the diatom *Grammonema cf. islandica*, which contains a B_{12}-independent methionine synthase (*METE*), a 15-fold increase in the expression of *METE* was observed when grown in the absence of B_{12} with no significant influence of iron status, suggesting *METE* expression can be driven by B_{12} status alone. Iron and B-vitamin amendment experiments with natural diatom assemblages in iron-limited waters of the Northeast Pacific Ocean provide evidence for vitamin-associated molecular responses that suggest elevated B_7 biosynthesis and the emergence of B_{12} limitation following iron addition. Furthermore B-vitamin gene modules comprised of partial and/or complete B-vitamin biosynthetic pathways in diatoms increased in response to iron addition, including genes potentially involved in the processing of B_{12} intermediates. Our results indicate that vitamins may play an important role in regulating phytoplankton growth and composition in this region, particularly following natural iron addition events.

Diatoms are responsible for approximately 20% of global carbon fixation each year and as much as 40% of marine organic carbon production (Nelson et al. 1996; Armbrust 2009). Over geologic timescales, it is hypothesized that varying rates of deep ocean carbon sequestration due to changes in diatom growth have influenced climate on a global scale (de Baar et al. 2005). Micronutrients such as iron are scarce enough to limit growth in vast areas of the ocean, called High-Nutrient, Low-Chlorophyll (HNLC) regions. These HNLC regions comprise approximately 30% of the ocean's surface waters and include large regions of the Southern Ocean, Equatorial Pacific, and Northeast Pacific Ocean (Boyd et al. 2007). During artificial iron fertilization, the introduction of bioavailable iron to HNLC waters creates diatom-dominated phytoplankton blooms with the potential to sequester large amounts of carbon in the seafloor sediments (de Baar et al. 2005; Boyd et al. 2007; Smetacek et al. 2012). Natural iron addition events occur when iron enters surface waters through aeolian transport, vertical mixing of the water column, inputs from coastal sediments and rivers, and active hydrothermal venting along fast and slow-spreading ridges (Moore et al. 2002; Saito et al. 2013). In HNLC waters of the Northeast Pacific Ocean, iron inputs from atmospheric dust and volcanic continental margins are major sources, with continental margin inputs fueling winter phytoplankton

*Correspondence: amarchetti@unc.edu

Additional Supporting Information may be found in the online version of this article.

blooms when dust deposition is low (Lam et al. 2006; Lam and Bishop 2008).

In addition to macro- and micro-nutrients, biosynthesized molecules such as B-vitamins serve as irreplaceable co-factors in enzymes and are required for proper cellular metabolism. These biologically-derived compounds may be growth-limiting to microorganisms unable to synthesize or acquire directly from the environment. It has been proposed that B-vitamins influence microbial community composition, where during bloom events, seawater may be depleted or enriched in vitamins consumed or produced by the blooming species, thereby influencing species succession by creating optimal environmental conditions for organisms producing the depleted vitamin and/or requiring the enriched vitamin (Provasoli 1963; Bertrand et al. 2007, 2015; Gobler et al. 2007; Sanudo-Wilhelmy et al. 2014). In particular, instances of iron and B_{12} co-limitation on phytoplankton growth have been documented in the Southern Ocean (Bertrand et al. 2007, 2011, 2015). These findings collectively support the notion that vitamin availability can be an important driver of phytoplankton community dynamics and primary productivity in marine environments.

B_7 is required as a cofactor in carboxylation enzymes, most notably those involved in fatty acid synthesis, and is produced through a series of reactions beginning with the compound pimeloyl-coenzyme A (Streit and Entcheva 2003). Four genes are involved in the B_7 biosynthetic pathway, which begins with the compound pimeloyl-CoA: *BIOF* (encoding KAPA synthase), *BIOA* (DAPA synthase), *BIOD* (dethiobiotin synthase), and *BIOB* (biotin synthase) (Webb et al. 2007). Orthologs for all genes are found in algae with the exception of *BIOD* (Croft et al. 2006). Because diatoms in culture are able to grow without B_7 added to the medium, it is assumed there is a *BIOD*-like homolog present that provides the end product of the BIOD reaction and the precursor to B_7, dethiobiotin. The last enzyme in the pathway, BIOB, is an iron-dependent enzyme containing multiple iron-sulfur clusters. The iron-sulfur clusters facilitate binding of dethiobiotin and donate a sulfur atom to the B_7 molecule itself (Jarrett 2005). Therefore, it is hypothesized that iron limitation in marine diatoms could alter the production, function, and activity of BIOB enzymes. Interestingly, in the yeast *Saccharomyces cerevisiae*, iron limitation causes a decrease in B_7 biosynthesis and activates a transporter that functions in the acquisition of external sources of B_7 (Shakoury-elizeh et al. 2004). If a similar mechanism for B_7 uptake is present in diatoms, this would allow intracellular iron in short supply to be redistributed towards other necessary iron-dependent processes, although such a mechanism has yet to be identified in diatoms.

B_{12}, or cobalamin, plays a major role in eukaryotic methionine synthesis as it is required in the B_{12}-dependent enzyme, methionine synthase (METH). Alternatively, some phytoplankton possess a B_{12}-independent methionine synthase (METE). Both forms of the enzyme catalyze the transfer of a methyl group from methyltetrahydrofolate to homocysteine, the final step in methionine biosynthesis (Pejchal and Ludwig 2005). While some eukaryotic phytoplankton have the ability to produce B_1 and B_7, there is no evidence for de novo eukaryotic B_{12} synthesis. Thus, these microorganisms must either alleviate their B_{12} demand (e.g., by possessing *METE*) or obtain it from their environment (Croft et al. 2005; Sanudo-Wilhelmy et al. 2014). B_{12} is an energetically costly molecule to synthesize, requiring approximately 21 enzymes (Warren et al. 2002). In eukaryotes, in addition to being used as a cofactor in METH, it is also utilized in succinyl Coenzyme A (CoA) production through methylmalonyl-CoA mutase. However, since this enzyme is found in diatoms that do not require B_{12}, it is not the primary determinant of B_{12} auxotrophy (Croft et al. 2006). Instead, there is a strong correlation between the absence of a functional *METE* gene and B_{12} auxotrophy among examined microalgae (Helliwell et al. 2011). The source of B_{12} to eukaryotic marine phytoplankton is from select prokaryotes, where 35% of marine bacteria with sequenced genomes have the full biosynthetic pathway (Sanudo-Wilhelmy et al. 2014). Recent studies have found various forms of B_{12} are biosynthesized by marine prokaryotes, with most photoautotrophic cyanobacteria likely producing only pseudocobalamin, a variant less bioavailable to marine eukaryotes as compared to cobalamin, which is produced by select heterotrophic bacteria and Thaumarchaeota (Helliwell et al. 2016; Heal et al. 2017). In addition, B_{12} availability may influence photosynthesis via production of phylloquinones, electron carriers involved in photosystem I, which require methionine for their synthesis (Lohmann et al. 2006). B_{12} limitation has been observed to increase cellular iron requirements of B_{12}-auxotrophic diatoms, potentially through increases in cytochromes and ferredoxins to replace phylloquinones produced through METH-dependent synthesis. It is hypothesized iron and B_{12} co-limitation could impair photosynthesis by reducing the availability of both iron- and methionine-dependent electron carriers (King et al. 2011).

Even when iron and B_{12} do not limit primary production, increases in iron can influence phytoplankton B_{12} consumption and bacterial B_{12} production (Bertrand et al. 2011). An analysis of diatom *METE* possession in available diatom transcriptomes indicates that 62% of Southern Ocean diatoms contain putative *METE*, compared to only 11% possession among diatoms in other regions of the ocean (Ellis et al. 2017). This suggests there may be a biogeographical basis for the presence of *METE*, in that phytoplankton may have reduced their B_{12} requirements where B_{12} availability is low and possibly growth limiting. Furthermore, B_{12} levels within coastal regions can influence community composition, as dinoflagellates have been observed to outcompete diatoms after B_{12} addition, creating a phytoplankton community that may be less likely to export carbon from the upper ocean

when compared to diatom-dominated communities (Koch et al. 2012; Agusti et al. 2015).

In this study, we investigated the influence of iron status on B_7 production, B_{12} utilization and *METE* activity in diatom isolates and natural assemblages from HNLC waters in the Northeast Pacific Ocean. We quantified the transcriptional response of *BIOB* under variable iron and B_7 growth conditions through targeted gene expression approaches in the oceanic diatom *P. granii*. In addition, gene expression of *METH* in the B_{12}-auxotroph *P. granii*, and *METH* and *METE* in *Grammonema cf. islandica*, an oceanic diatom without a B_{12} requirement, were measured in response to variable iron and B_{12} status. This laboratory work complements previous studies investigating the influence of external B_{12} scarcity on *METH* and *METE* gene expression within laboratory cultures of model coastal diatom species *Phaeodactylum tricornutum* and *Thalassiosira pseudonana* (Bertrand et al. 2012). Even more importantly, our laboratory studies serve as a basis for interpreting natural assemblage metatranscriptomic responses to iron/B_{12} and iron/B_7 incubation experiments performed at Ocean Station Papa (OSP) in the Northeast Pacific Ocean. Iron and B-vitamin dynamics are explored in order to better understand how naturally occurring iron fertilization events could influence B-vitamin production and consumption and ultimately phytoplankton community growth and composition.

Methods

Culture conditions

The pennate diatoms *P. granii* (UNC1102) and *Grammonema cf. islandica* (UBC1301) used in the laboratory experiments were isolated from OSP (50°N, 145°W) located in the Northeast Pacific Ocean in 2011 and 2013, respectively. Only *P. granii* was used for B_7 experiments. Both species were used for B_{12} experiments: *P. granii* is auxotrophic for B_{12} and *G. cf. islandica* is facultative, possessing *METE* (Ellis et al. 2017). *G. cf. islandica* was identified based on a 99% homology to an 18S rDNA sequence deposited in Genbank (accession number AJ535190).

Diatom cultures were maintained in the artificial seawater medium Aquil using trace metal clean (TMC) techniques according to Marchetti et al. (2006). Cells were grown in 28 mL acid-cleaned polycarbonate centrifuge tubes for a minimum of three growth cycles while in exponential phase ($\geq$ 18 cell divisions) in order to pre-acclimate cells to treatment conditions before use in large experimental cultures, with the exception of *P. granii* under B_{12} limitation and *G. cf. islandica* under iron limitation (*see* below). Macronutrients were added to Aquil medium in final concentrations of 300 μmol L^{-1} NO_3^-, 10 μmol L^{-1} PO_4^{3-}, and 100 μmol L^{-1} $Si(OH)_4$. Media were dispensed into 2 L acid-cleaned, Milli-Q H_2O-rinsed polycarbonate bottles and supplemented with filter-sterilized (0.2-μm Acrodisc) trace metals, vitamins, and iron bound to EDTA in a 1 : 1 ratio. Growth-replete vitamin treatments (+B_7 or +B_{12}) were added in concentrations established for Aquil medium: 297 nmol L^{-1} B_1, 2047 pmol L^{-1} B_7, 348 pmol L^{-1} B_{12} (Price et al. 1989). For treatments where B_7 was absent from the media (−B_7), all vitamins except B_7 were added in Aquil concentrations, and likewise within treatments where B_{12} was absent (−B_{12}), all vitamins except for B_{12} were added to growth media.

In iron-replete treatments (+Fe), Aquil was buffered with 100 μmol L^{-1} EDTA, yielding 1370 nmol L^{-1} of total iron, corresponding to ca. 2.7 nmol L^{-1} of unchelated dissolved iron (Marchetti et al. 2009). In order to iron limit the growth rate of *P. granii*, the iron chelator desferroxiamine B (DFB) was used in Fe : DFB ratios of 1.5 : 200 nmol L^{-1}, yielding an unchelated iron concentration of ca. 0.02 pmol L^{-1} (Strzepek et al. 2012). The Fe : DFB solution was allowed to equilibrate overnight before being added to medium. For *G. cf. islandica*, iron limitation of growth rate was achieved by adding premixed Fe-EDTA (1 : 1) at total iron concentrations of approximately 6.24 nmol L^{-1}, yielding an unchelated iron concentration of 12 pmol L^{-1}. The +Fe and iron-limited (−Fe) medium was allowed to chemically equilibrate overnight before use.

Four laboratory treatments were prepared to test the physiological and molecular responses of *P. granii* to varying iron/B_7 conditions: (1) +Fe/+B_7; (2) +Fe/−B_7; (3) −Fe/+B_7; and (4) −Fe/−B_7. Laboratory treatments prepared to test the response of *P. granii* and *G. cf. islandica* to iron/B_{12} conditions consisted of the following treatments: (1) +Fe/+B_{12}; (2) +Fe/−B_{12}; (3) −Fe/+B_{12}; and (4) −Fe/−B_{12}. All experiments were inoculated when seed cultures were in mid-exponential growth phase, except in the cases of B_{12}-limited *P. granii* and iron-limited *G. cf. islandica*. Because *P. granii* growth ceased after approximately two transfers in −B_{12} medium regardless of antibiotic treatment, +B_{12}-grown *P. granii* cultures (18 mL) were used as the inoculum for the −B_{12}/+Fe and −B_{12}/−Fe treatments. A similar procedure was used to grow iron-limited *G. cf. islandica*. Exponential phase cultures were transferred from 8.59 nmol L^{-1} medium into medium containing a slightly lower iron concentration of 6.24 nmol L^{-1}.

All cultures were grown under a continuous, saturating photon flux density of 110 μmol photons m^{-2} s^{-1}, with the exception of three iron-replete, light-limited *P. granii* cultures (+Fe/+B_7/LL) used as a reduced-growth rate comparison to iron-limited *P. granii* cultures. Light-limitation was achieved by growing these cells under a light intensity of 40 μmol photons m^{-2} s^{-1}. The length of experiments varied among diatom species and experimental treatments, but was typically between 5 d and 15 d. Cultures were maintained at 12°C and mixed on a stir plate for the duration of the pre-acclimation and experimental period in order to prevent cells from settling. Subsamples were taken daily to monitor changes in cell biomass via fluorescence measurements and

to ensure cells remained in the exponential phase of growth throughout the duration of the culture period.

Growth rates combined with photophysiology served as indicators of iron and vitamin stress or limitation. Exponential-phase growth rates (μ) were determined from in vivo chlorophyll *a* (Chl *a*) fluorescence using a Turner Designs model 10-AU fluorometer (in vivo chlorophyll optical kit). Growth rates were calculated while cultures were in mid-exponential phase using the linear regression of the natural log of Chl *a* fluorescence vs. time as described in Marchetti and Harrison (2007). In our *P. granii* cultures, the r^2 values of in vivo fluorescence vs. cell concentration derived from light microscopy counts were >0.9 for both iron-limited and iron-replete treatments, demonstrating fluorescence was proportional to cell concentrations.

Estimates of photophysiology ($F_v : F_m$) were obtained by measuring fluorescence induction with a Satlantic FIRe fluorometer (Gorbunov and Falkowski 2005). Before each measurement, a subsample (5 mL) of each culture was placed in the dark for 20 min. A short, saturating pulse of blue light (450 nm) was applied to dark-acclimated phytoplankton for a 100 μs duration to measure fluorescence induction from minimum (F_o) to maximum (F_m) fluorescence yields. F_o and F_m were used to estimate $F_v : F_m$ from $(F_m - F_o)/F_m$. Values were calculated for each culture upon harvesting during the mid-exponential growth phase. Iron/B_{12} culture measurements were obtained using single-turnover flash, while iron/B_7 measurements were performed using multiple-turnover flash, which resulted in the differences in ranges of $F_v : F_m$ observed between experiments (Behrenfeld and Milligan 2013; Kromkamp and Forster 2003). Relative decreases in $F_v : F_m$ due to iron limitation remained apparent within each set of experiments.

Iron addback experiments

To further investigate whether iron status triggers transcriptomic regulation of B_7 production genes, an iron addback experiment was performed on a 2 L iron-limited *P. granii* culture with B_7 present in the growth medium. Growth rates were recorded to ensure iron limitation and monitor the response to iron addition. Upon early exponential phase, 1.5 L of culture was harvested on 3 μm polycarbonate filters and stored at -80°C until RNA extraction. Approximately 49 μL of 1.4×10^{-2} M Fe : EDTA (1 : 1) was added to the remaining 500 mL of $-$Fe/+B_7 cells to achieve a final iron concentration of 1370 nmol L^{-1}. Upon reaching mid-exponential phase, all but 1 mL of the culture was harvested for RNA extraction and $F_v : F_m$ determination. The remaining 1 mL fraction of the exponentially growing culture was used to inoculate a +Fe/+B_7 1 L culture in order to serve as a longer-term addback comparison. This post addback culture was harvested in mid-exponential phase after 6 d and samples were again collected for $F_v : F_m$ and RNA.

Changes in gene expression of methionine synthase genes (*METH* and *METE*) in response to short-term iron addition were assessed for *P. granii* (*METH* only) and *G. cf. islandica* by performing an iron addback to previously iron-limited 1 L cultures. During early exponential growth phase, $F_v : F_m$ was obtained and then 400 mL of iron-limited cells were filtered for RNA. Approximately 49 μL of 1.4×10^{-2} M Fe : EDTA (1 : 1) was then added to the remaining cells immediately following the first filtration to achieve a final iron concentration of 1370 nmol L^{-1}. Cultures were incubated for an additional 24 h before the same set of measurements were obtained using the remainder of the culture. +Fe/+B_{12} and +Fe/$-B_{12}$ cultures were grown using the same protocol but without iron addback and subsequent second filtration. Before the final filtration of all cultures, a 2 mL subsample was collected to check for bacterial contamination using the SYBR-stain method described below.

Axenic culture conditions for iron/B_{12} experiments

Antibiotic-treated cultures were prepared by adding an antibiotic cocktail consisting of 50 μg mL^{-1} streptomycin, 100 μg mL^{-1} ampicillin, 67 μg mL^{-1} gentamycin, 20 μg mL^{-1} ciprofloxacin, and 2.2 μg mL^{-1} chloramphenicol. Antibiotics were added to 5 mL of cell culture and incubated for 24 h before a 1 mL aliquot was transferred into fresh sterile Aquil medium of the corresponding treatment (+/$-$Fe, +/$-B_{12}$). Following equilibration to medium, bacterial presence was detected by the use of bacteriological peptone broth in conjunction with SYBR green staining and epifluorescent microscopy (Noble and Fuhrman 1998). Cultures were deemed low or free of bacteria when bacteriological peptone broth remained clear after 3 d and a substantial reduction in bacterial cells could be observed following SYBR staining. The reduction in bacteria was quantified by performing cell counts using Olympus Metamorph Basic v.7.6.0.0 software's integrated morphometry analysis on 10 randomly chosen fields of view from each SYBR-stained filter, which were then averaged. In all cultures, bacterial abundances were substantially reduced (93–99%) after incubation with antibiotics.

Targeted gene expression analysis

RNA extractions were performed on frozen filters using the RNAqueous 4-PCR kit (Ambion). In order to remove DNA contamination, RNA was then incubated with deoxyribonuclease (DNase) I at 37°C for 45 min and purified by DNase inactivation reagent (Ambion). RNA concentrations were measured using a NanoDrop spectrophotometer and samples with concentrations <250 ng μL^{-1} were concentrated using the RNeasy MinElute Cleanup Kit (Qiagen). Quantitative PCR (qPCR) with the RNA samples was used to determine DNA contamination levels, with samples containing >10 DNA copies per mL of RNA given additional incubation and purification with DNase I. Two micrograms of total RNA was reverse transcribed using the SuperScript III

First-Strand cDNA Synthesis kit with oligo-dT primers (Invitrogen).

P. granii BIOB primers were designed from a *BIOB* partial gene sequence obtained from an expressed sequence tag (EST) library (Marchetti et al. 2012) to target a 189 bp region, within the size range suitable for qPCR analysis (< 250 bp). *P. granii ACT* and *METH* primers were previously designed from ESTs (Marchetti et al. 2015; Ellis et al. 2017). *G. cf. islandica METH*, *METE*, and *ACT* primers for qPCR were designed from gene sequences obtained from the *G. cf. islandica* transcriptome to target 183 bp, 172 bp, and 175 bp regions, respectively. Primers were developed using Primer 3 and tested using PCR, gel electrophoresis, and PCR product sequencing (Supporting Information Table 1). Actin was chosen as the housekeeping gene as its expression has been reported to remain stable during varying physiological states in diatoms (Alexander et al. 2012). Standards were created for quantification purposes by PCR amplification at 94°C for 2 min, followed by 40 cycles of 30 s at 95°C, 30 s at the specific primer's annealing temperature, and 1 min at 72°C. Reactions consisted of 1 μL DNA, 1 μL Taq Buffer, 1 μL $MgCl_2$, 0.5 μL dNTP, 0.4 μL of forward and reverse primers, 0.075 μL Taq polymerase, and 4.625 μL UV-treated water. Amplified fragments were cloned and transformed into *Escherichia coli* using the TOPO TA Cloning Kit (Life Technologies). Colonies containing the cloned gene fragment were incubated at 37°C overnight in liquid Luria broth media, and plasmids were extracted using the QIAprep Spin Miniprep Kit (Qiagen). Plasmids were linearized by incubation with *SpeI* at 37°C for 1 h and enzyme denaturation at 80°C for 20 min. Linearized plasmids were quantified with a Qubit using the Qubit RNA Assay Kit (Life Technologies) to create a set of standards for each gene of interest ranging between 10^1–10^6 copies μL^{-1}. Copies per μL of cDNA were determined by performing triplicate 20 μL qPCR reactions with a Mastercycler ep gradient S (Eppendorf) on each sample and normalizing each gene to actin (*ACT*) expression from the same sample. Reactions were composed of 2 μL DNA standard or cDNA unknown, 10 μL SyberFast Universal qPCR mastermix (Kapa), 4.8 μL Milli-Q water, and 1.6 μL each of the forward and reverse primers.

Statistical analyses

To test for significant differences in growth rates, $F_v : F_m$ values, and gene expressions among iron/B_7 treatments, a one-way ANOVA was used followed by Tukey multiple comparison tests. To test for significant differences between iron/B_{12} treatments, two-tailed homoscedastic *t*-tests within each species were performed on growth rate, gene expression and $F_v : F_m$ values. Significant differences in Chl *a*, $F_v : F_m$, and diatom densities among incubation treatments was determined through one-way RM ANOVA followed by Holm-Sidak comparison tests. The level of statistical significance for all tests was $p < 0.05$. All tests were performed in Sigmaplot v12.5 (Systat Software).

Field experimental design and RNA extraction

Near-surface seawater was collected onboard the CCGS John P. Tully from June 07–25th 2013 as a part of the Line-P program that transects coastal to open ocean waters in the subarctic Northeast Pacific Ocean. Samples were collected at stations P2 (48°36N, 126°00W), P4 (48°39N 126°40W), P12 (48°58.2N, 130°40W), P16 (49°17N, 134°40W), P20 (49°34N, 138°40W), and P26 (OSP; 50°N, 145°W). At each station, samples for size-fractionated Chl *a*, dissolved nutrients and dissolved vitamin concentrations, flow cytometry and phytoplankton preservations were collected (detailed methods of each measurement are provided below). At OSP, microcosm iron and B_7/B_{12} enrichment experiments were conducted. Seawater was collected from a depth of 10 m, corresponding to 33% surface irradiance, using a TMC sampling system consisting of Teflon tubing connecting to an air bellows pump as described in Marchetti et al. (2012). Seawater was pumped directly into a positive-pressure laminar flow hood and used to rinse and fill TMC cubitainers. Prior cleaning procedures for the cubitainers included 1.2 mol L^{-1} hydrochloric acid (reagent grade) soaking for 3 d followed by three rinses with Milli-Q water, soaking with 1.2 mol L^{-1} hydrochloric acid (trace metal grade) for 1 week, three rinses with Milli-Q, and finally a 0.1 mol L^{-1} acetic acid (trace metal grade) soak. Immediately before use, cubitainers were rinsed three times with ambient low-iron OSP seawater. Approximately 30 L of seawater was immediately collected for initial measurements, and served as the initial time point (T_0).

Cubitainers ($\sim$ 10 L) were prepared in triplicate for each treatment and incubated for 96 h. The following treatments were performed: 4 nmol L^{-1} iron chloride (Fe), 200 pmol L^{-1} biotin (B_7), 200 pmol L^{-1} cyanocobalamin (B_{12}), 4 nmol L^{-1} iron chloride and 200 pmol L^{-1} biotin (FeB_7), and 4 nmol L^{-1} iron chloride and 200 pmol L^{-1} cyanocobalamin (FeB_{12}). Three cubitainers received no additions and served as an unamended control (Ctl). Cubitainers were placed in two on-deck Plexiglass incubators and cooled with flow-through seawater at 33% irradiance for 96 h. Subsamples from each cubitainer were collected following the 96 h incubation and used for measurements of size-fractionated Chl *a*, diatom cell counts, $F_v : F_m$ and RNA.

Seawater (9 L) for RNA analysis was filtered directly from each cubitainer onto Supor Pall 0.45 μm porosity filters (142 mm) using a peristaltic pump. Filters were wrapped in aluminum foil and immediately flash frozen in liquid nitrogen. Samples were later transferred to storage in −80°C freezers until RNA extractions were performed. Filters were briefly thawed on ice before being extracted individually using the ToTALLY RNA Kit (Ambion). The extraction procedure followed manufacturer protocols with the modified first step of glass bead addition in order to facilitate disruption of cells.

Removal of DNA was performed with DNase 1 (Ambion) followed by qPCR on total RNA to ensure DNA contamination was not present in total RNA samples.

Physiological assessment: Chl *a*, $F_v : F_m$, cell counts, bacterial counts

For estimates of size-fractionated Chl *a*, 300 mL of seawater was vacuum filtered through a 5 μm pore-sized polycarbonate filter, and the filtrate was re-passed through a GF/F filter (0.7 μm pore size). Filters were frozen at −80°C until analysis. Chl *a* extraction was performed in the laboratory using 90% acetone at −20°C overnight and concentrations were determined fluorometrically using a Turner Designs 10-AU fluorometer (Brand et al. 1981). While it is true that Chl *a* content varies by taxa and with changes in cellular physiology (thus affecting the C : Chl *a* cellular ratio), Chl *a* is a relatively good proxy for phytoplankton carbon concentrations at values above 0.14 μg L^{-1}, and therefore Chl *a* concentrations are interpreted as an equivalent measurement to phytoplankton biomass (Behrenfeld et al. 2005). Photophysiology measurements were performed on a bench-top fast repetition rate fluorometer (Solience Instruments). Background fluorescence blanks were prepared by syringe filtering < 5 mL of seawater through a GF/F filter. A single turnover (ST) fluorescence induction protocol (100 flashlets with 1.0 μs length and 2.5 μs interval, 46,200 μmol quanta m^{-2} s^{-1} peak power intensity, providing ~ 5–10 quanta per RCII in 250 μs) was applied. The fluorescence yields F_o and F_m were estimated from the mean of 22 consecutive ST acquisitions. In the study region, iron addition has been shown to increase the $F_v : F_m$ of phytoplankton communities from less than 0.4 to approximately 0.6 (Schuback et al. 2015).

Diatom cell densities were estimated by preserving 250 mL of seawater with 4% Lugol's solution in amber glass bottles and kept in the dark until analysis. In the laboratory, 50–100 mL of the preserved samples were settled in Utermöhl settling chambers for at least 24 h. Diatom cell counts were performed via light microscopy and at least 10 fields of view were counted. Cell counts were determined based on volume settled, magnification used, and slide area. Diatoms were sorted into one of the following groups: (1) *Pseudo-nitzschia* (large; >20 μm in length), (2) *Pseudo-nitzschia* (small; < 20 μm in length), (3) centrics, and (4) other pennates. "Centrics" included both large and small centrics, e.g., *Proboscia* sp., and *Chaetoceros* sp. "Other pennates" included pennates visually distinct from *Pseudo-nitzschia*.

To measure bacterial cell densities along the Line-P transect, 2 mL surface seawater was collected and preserved using a 10% flow cytometry preservative cocktail consisting of 40% phosphate-buffered saline solution (PBS), 10% formalin, and 0.5% glutaraldehyde. Samples were refrigerated at 4°C for 15 min to allow for fixative to permeate membranes before being flash frozen with liquid nitrogen and stored at −80°C until analysis. Thawed fractions were injected into a Becton Dickson FACSCalibur flow cytometer (San Jose, California). Total bacteria were targeted using a SYBR green stain fluorescing at 530 nm. *Synechococcus* populations were captured via fluorescence at 585 nm, with the addition of alignment beads for calibration. *Prochlorococcus* was not detected in any of the samples. FlowJo v7.6.5 was used for quantitative analysis (Johnson et al. 2010). Total bacterial populations subtracted from the cyanobacteria populations are referred to as non-photosynthetic (non-ps) bacteria.

Dissolved vitamins

For determination of dissolved B-vitamin (B_1 [thiamine hydrochloride], B_2 [riboflavin], B_6 [pyridoxal hydrochloride], B_7 [biotin], and B_{12} [cyanocobalamin]) concentrations, duplicate 2 L seawater samples from 5 m depth were collected during the day using rosette Niskins at stations P2, P4, P12, P16, P20, and OSP along the Line-P transect. Seawater was filtered using a sterile, methanol-cleaned Whatman Polycap AS 0.2 μm porosity filter into dark HDPE bottles and frozen at −20°C onboard the vessel. Samples were shipped on dry-ice and stored at −80°C until pre-concentration in the laboratory.

Vitamin preconcentration was performed via a solid phase extraction (SPE) technique developed by Sañudo-Wilhelmy et al. (2012). Briefly, Bondesil-C18 resin (Agilent) was prepared by mixing with reagent grade methanol in a 1 : 1 ratio to create a resin slurry. Next, a series of two rinses was performed on the resin by allowing particles to settle, decanting off the methanol, and resupplying fresh methanol. Resin was subsequently rinsed with Milli-Q water in the same manner three times, and 6–7 mL of this 1 : 1 resin : water slurry was packed into polypropylene chromatography columns (Bio-Rad). Resin columns were further conditioned by passing through 20 mL High Performance Liquid Chromatography (HPLC) grade methanol, 20 mL of pH adjusted 6.5 Milli-Q, followed by 20 mL of seawater sample adjusted to pH 6.5. These seawater samples were thawed overnight and acidified to a pH of 6.5 with 6 M hydrochloric acid. Following resin conditioning, the remainder of seawater samples was passed through the columns at a rate of approximately 1 mL min^{-1} in the dark at room temperature. Seawater was subsequently acidified to a pH of 2 and re-passed through the resin, again under dark conditions at room temperature. All vitamins aside from biotin are bound to resin at pH of 6.5, while biotin requires a pH of 2 in order to more effectively bind resin. Significant loss of vitamin fractions over the duration of the resin passing has not been observed using this method, and the vitamin fractions appear to be stable at room temperature given our satisfactory spike recoveries (*see* below). The only vitamin found to be light sensitive was riboflavin, and to minimize loss, the pre-concentrations were performed in the dark. Column resin pH was neutralized by passing through 30 mL of pH 7 Milli-Q water. The addition of water

to the resin column does not cause elution to occur and is solely for removal of salt that could interfere in the liquid chromatography-mass spectrometry (LC/MS) quantification.

Immediately before analysis, samples were eluted with 10 mL of methanol, dried under vacuum at 40°C, and dissolved in 250 mL of LCMS water (pH adjusted to 6.5). Standard addition was performed on every sample in order to account for matrix effects and prepare a five-point standard curve. Negative and positive controls consisted of a blank (comprised of only 2 L synthetic seawater, no vitamins added) and a spike (1 pmol L^{-1} spike of each B-vitamin into synthetic seawater), respectively. LC/MS analysis was performed with a Thermo TSQ Quantum Access triple quadrupole mass spectrometer with electro-spray ionization and a Thermo Accela High Speed Liquid Chromatography set-up using LC/MS water as the injection solvent (Sañudo-Wilhelmy et al. 2012). Excalibur software was used for computational quantitative analysis. Instrumental detection limits were used due to traditional analytical detection limits based on 3X-standard deviation of the procedural blank being essentially zero. The instrumental detection limits are defined as 3X-standard deviation of the lowest detectable concentration of standard used for each vitamin, and were as follows: 0.25 pmol L^{-1} for thiamine hydrochloride and biotin, 0.13 pmol L^{-1} for riboflavin and cyanocobalamin, and 0.38 pmol L^{-1} for pyridoxal hydrochloride. SPE recoveries were determined by dividing the amount measured via LC/MS (multiplied by the concentration factor) by the amount added in the spiked control: 100% for thiamine hydrochloride, 63% for riboflavin, 75% for pyridoxal hydrochloride, 180% for biotin, and 72% for cyanocobalamin. These recoveries are comparable to those obtained in previous vitamin studies even with much lower spike concentrations used (Sañudo-Wilhelmy et al. 2012; Heal et al. 2014). The high biotin recovery indicates up to 1 pmol L^{-1} of biotin contamination may have been introduced via reagents used in the seawater preconcentration procedure. Therefore, biotin concentrations reported may be artificially slightly higher than naturally occurring along the Line P transect.

Metatranscriptomic sequencing analysis

For metatranscriptomic sequencing, mRNA in each sample was concentrated using the Poly(A)Purist MAG Kit (Ambion) followed by library preparation with the Illumina TruSeq Stranded mRNA Library Preparation Kit and HiSeq v4 reagents. To obtain sequences for all incubations, RNA was pooled by treatment for all triplicate samples (duplicate for the control). Sequencing of barcoded samples was performed on a single lane on an Illumina HiSeq 2000 (125 bp, paired-end). Sequencing statistics are provided in Supporting Information Table 2. Raw sequences are deposited in the Sequence Reach Archive (SRA) database under accession number SRP074366.

Raw reads were trimmed for quality bases and removal of adapters using Trimmomatic v0.32 (paired-end mode, adaptive quality trim with 40 bp target length and strictness of 0.6, minimum length of 36 bp; Bolger et al. 2014). Trimmed paired reads were merged into single reads with BBMerge v8.0. The resulting merged pairs and non-overlapping paired-end reads were assembled using ABySS v1.5.2 with a multi-kmer approach (Birol et al. 2009). Assemblies were merged to remove redundant contigs using TransABySS v1.5.3 (Robertson et al. 2010). Read counts were obtained by mapping raw reads to contigs with Bowtie2 v2.2.6 (end-to-end alignment; Langmead and Salzberg 2012; Supporting Information Table 2). Alignments were filtered by mapping quality score (MAPQ) of 10 or higher as determined by SAMtools v1.2 (Li et al. 2009). Taxonomic and functional annotations were assigned based on sequence homology via BLASTx v2.3.0 with an E-value cutoff of 10^{-3} (Altschul et al. 1990). Functional annotations were assigned using the Kyoto encyclopedia of genes and genomes (KEGG; Release 75), while taxonomic assignments were obtained with MarineRefII (Laboratory of Mary Ann Moran, University of Georgia), a custom-made database comprised of protein sequences of marine microbial prokaryotes and eukaryotes including all sequenced transcriptomes from the Marine Microbial Eukaryote Transcriptome Sequencing Project (MMETSP; Keeling et al. 2014). Taxonomic information was obtained from the National Center for Biotechnology Information's (NCBI) Taxonomy Database (each isolate in MarineRefII is assigned a NCBI taxonomic ID). The information from NCBI was manually curated to ensure proper assignment and use of common phytoplankton taxonomic ranks.

All diatom-assigned counts were summed by genus and KEGG Orthology (KO). For genes without KO assignments but possessing an annotated gene definition (e.g., *CBA1*, *ISIP2A*, *ISIP2B)*, raw counts corresponding to KEGG gene definitions were summed. edgeR v3.12.0 was used to calculate normalized fold change and counts-per-million (CPM) from pairwise comparisons (Robinson and Smyth 2008; Robinson et al. 2010). For pathway-level analysis, read counts corresponding to KOs contained within each KEGG vitamin biosynthetic module were summed. Heatmaps were produced with the R package pheatmap v1.0.8, and the dendrogram was created using the default settings of Euclidean distance and hierarchical clustering. MA plots with taxonomic pies were created with edgeR output and a custom script available at www.github.com/marchettilab/mantaPlot. Assembled contigs, functional and taxonomic annotations, and read counts are available at https://marchettilab.web.unc.edu/data/.

Results

BIOB gene expression in response to iron limitation within laboratory cultures

Iron-replete *P. granii* cultures grew at a specific rate of 1.7 ± 0.04 d^{-1} while iron-limited cultures maintained a specific growth rate of approximately 0.6 ± 0.08 d^{-1}, resulting

in a 65% reduction in maximum growth rate (Fig. 1A; $p < 0.001$). There was no significant difference in growth rate between cultures with and without B_7 added to the growth media, either under iron-replete or iron-limited conditions. Assessment of $F_v : F_m$ further supports a physiological response to iron treatment and a negligible effect of external B_7 on photophysiology as iron-replete cultures maintained an $F_v : F_m$ of approximately 0.71 ± 0.002 while iron-limited cultures exhibited ratios of approximately 0.59 ± 0.01, an approximate 17% reduction (Fig. 1B; $p < 0.036$).

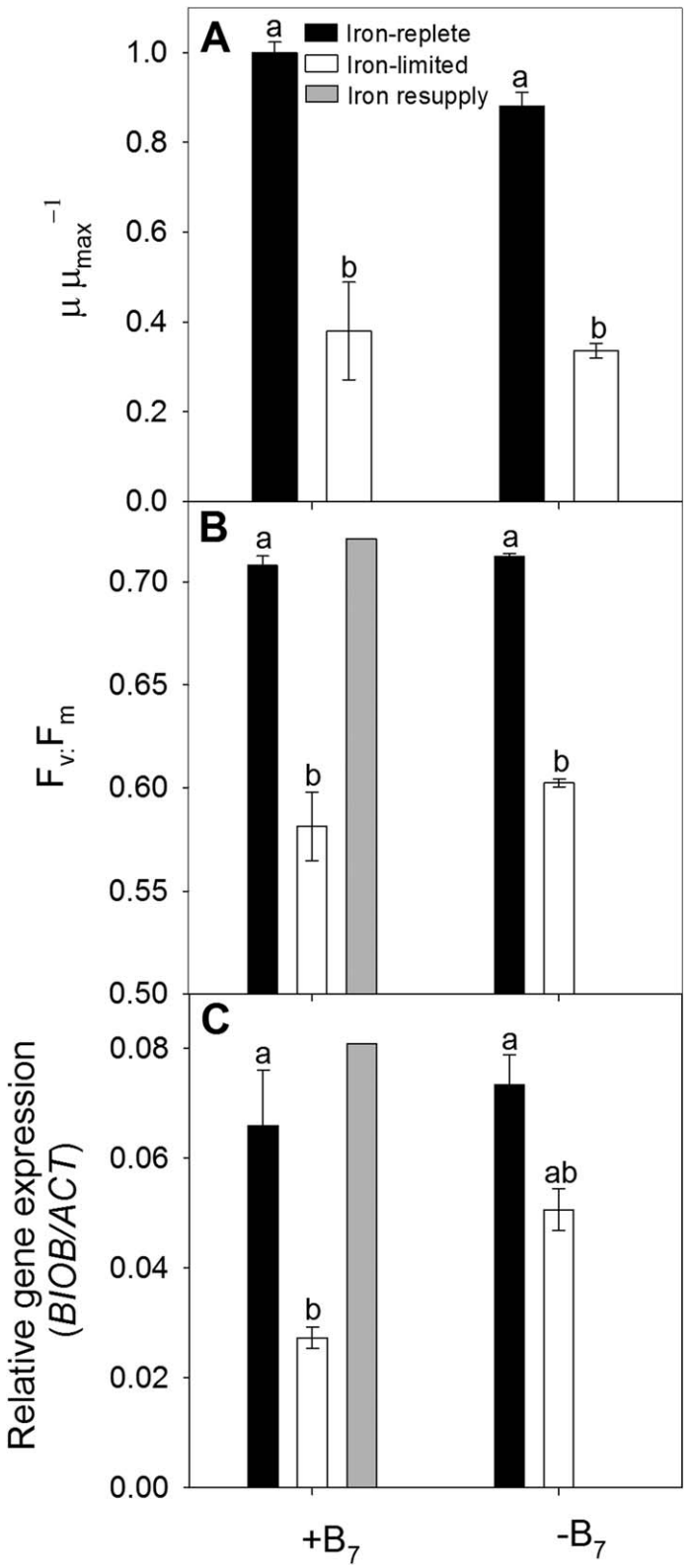

Fig. 1. *P. granii* growth rates, $F_v : F_m$, and *BIOB/ACT* gene expression as a function of iron and B_7 status. (**A**) Relative growth rates compared to the maximum growth rate (μ_{max}), (**B**) Maximum photochemical yield of PSII ($F_v : F_m$), and (**C**) Relative gene expression of biotin synthase normalized to actin (*BIOB/ACT*) of iron-replete (+Fe), iron-limited (−Fe) and iron resupplied *P. granii* in the presence (+B_7) or absence (−B_7) of vitamin B_7. Letters denote significant differences among treatments as determined via one-way ANOVA and Tukey multiple comparison tests ($p < 0.05$). Error bars represent ±1 standard error associated with the mean ($n = 3$, except in the iron resupply experiment where $n = 1$).

Relative *BIOB* gene expression, obtained by normalizing *BIOB* to *ACT* transcripts (*BIOB/ACT*), indicated an approximate 2-fold decrease in −Fe/+B_7 relative to the +Fe/+B_7 treatment (Fig. 1C; $p = 0.017$). *BIOB* expression in −Fe/−B_7 was also reduced although not significantly different from either the +Fe/+B_7 ($p = 0.49$), or −Fe/+B_7 ($p = 0.2$). Iron resupply experiments showed an increase in *BIOB* expression following the addition of iron to −Fe/+B_7 cells, with expression levels increasing > 3-fold over the duration of 6 d (Fig. 1C).

Light-limitation, in which cultures were grown under 40 μmol photons m^{-2} s^{-1}, resulted in a significantly reduced growth rate as compared to control cultures exposed to growth-saturating light conditions (110 μmol photons m^{-2} s^{-1}; Supporting Information Fig. 1A; $p = 0.02$). *BIOB* expression levels were not significantly different between the low-light (+Fe/+B_7/LL) treatment and +Fe/+B_7 ($p = 0.057$), suggesting the observed decrease in *BIOB* expression under iron limitation is not a general response to a reduction in growth rate (Supporting Information Fig. 1B).

METE and *METH* gene expression in response to iron limitation within laboratory cultures

P. granii iron-replete cultures with B_{12} supplied in the media (+Fe/+B_{12}) grew at 0.85 ± 0.11 d^{-1}, while iron-limited cultures (−Fe/+B_{12}) had reduced growth rates by 50% (0.45 ± 0.10 d^{-1}; $p = 10^{-3}$). *P. granii* cultures without B_{12} supplied in the medium were not able to survive more than two transfers (*see* methods). $F_v : F_m$ analysis supports a physiological response to iron limitation with a 40% decrease in $F_v : F_m$ within iron-limited treatments, regardless of B_{12} status (Supporting Information Fig. 2B; $p < 0.004$). Gene expression analysis of *METH* (*METH/ACT*) demonstrates a > 3-fold increase in the absence of B_{12} (+Fe/−B_{12}) relative to B_{12}-replete cultures (Fig. 2A; +Fe/+B_{12}: $p = 0.001$; −Fe/+B_{12}: $p = 0.0008$; and +B_{12}/Fe resupply: $p = 0.007$). *P. granii* has

previously been found to increase *METH* expression in the absence of B_{12} (Ellis et al. 2017). Here, we report that iron has no significant effect on *METH* expression with or without B_{12} in the medium.

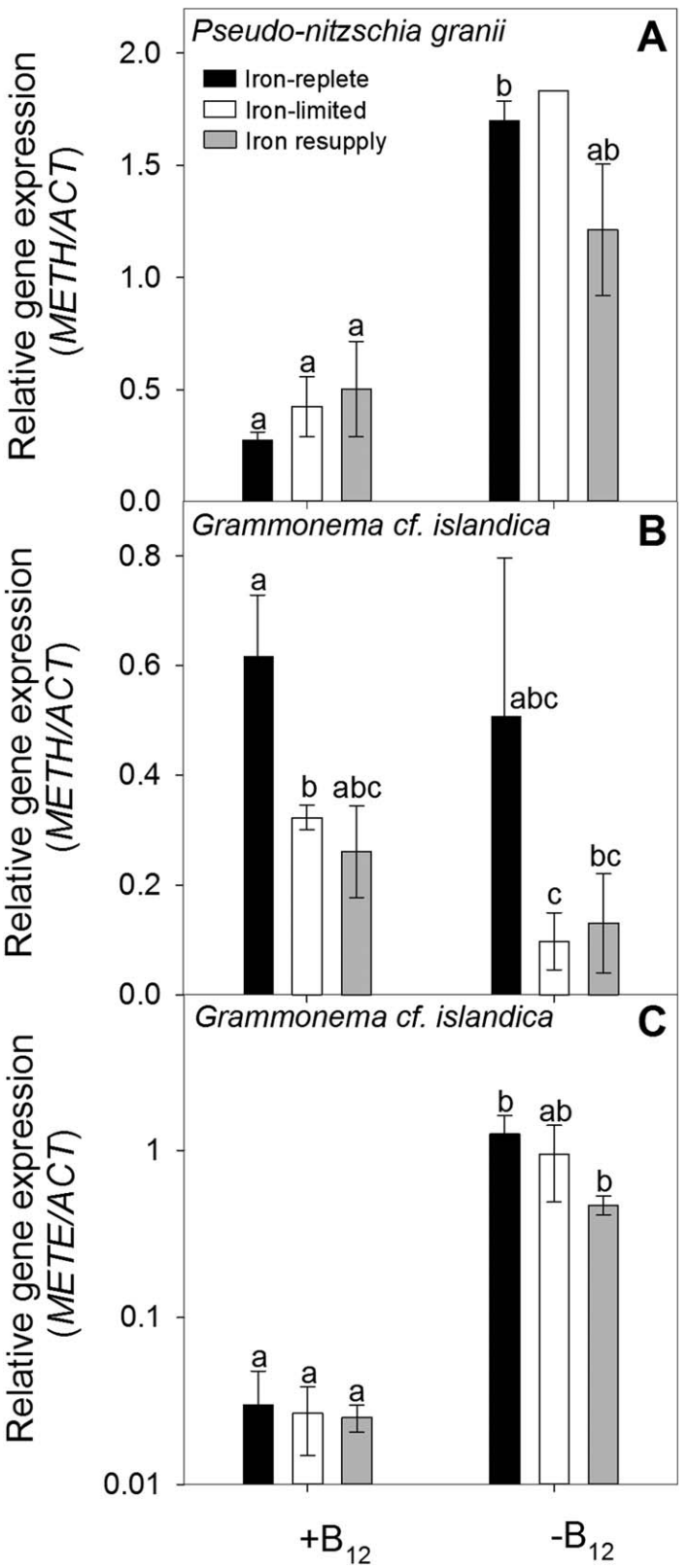

G. cf. islandica iron-replete cultures with B_{12} supplied in the medium (+Fe/+B_{12}) grew at approximately 0.88 ± 0.19 d^{-1}, while iron-limited cultures (−Fe/+B_{12}) experienced a 67% reduction in growth (0.29 ± 0.12 d^{-1}; $p = 0.004$; Supporting Information Fig. 2C). B_{12} absence (+Fe/−B_{12}) significantly decreased growth rates by 35% as compared to +Fe/+B_{12} conditions with cultures experiencing growth rates of 0.57 ± 0.08 d^{-1}. Furthermore, iron-limited cultures without B_{12} present (−Fe/−B_{12}) grew at significantly reduced rates as compared to their iron-replete counterparts, at approximately 0.35 ± 0.02 d^{-1} ($p = 0.014$). F_v : F_m decreased in iron-limited *G. cf. islandica* by 27%, with −B_{12} cultures having a negligible effect (Supporting Information Fig. 2D; $p < 0.002$). B_{12} absence decreased *G. cf. islandica METH* expression by 3-fold, as observed between −Fe/+B_{12} and −Fe/−B_{12} treatments ($p = 0.007$). Furthermore, *METH/ACT* expression was significantly influenced by iron status, with expression decreasing by > 2-fold under iron-limited conditions (−Fe/+B_{12} and −Fe/−B_{12}) when compared to iron-replete treatments (+Fe/+B_{12}; $p = 0.03$ and 0.02 respectively; Fig. 2B). It remains unclear whether *METH* expression in *G. cf. islandica* is indirectly influenced by growth rate or directly affected by iron availability. In contrast, *METE/ACT* expression was primarily affected by B_{12} status with no significant differences due to iron treatment; there was a > 15-fold increase in expression in −B_{12} cells (+Fe/−B_{12}; −B_{12}/Fe-resupply) when compared to treatments containing B_{12} ($p < 0.03$; Fig. 2C).

Growth dynamics and B-vitamin patterns along the Line-P transect

Trends along the natural iron gradient of the Line-P transect indicate phytoplankton biomass decreased whereas dissolved nitrate concentrations increased with distance from the shore (Fig. 3A). Larger phytoplankton (> 5 μm) decreased in biomass 7-fold from 1.85 ± 0.03 μg Chl *a* L^{-1} at the most coastal station (P2) to 0.26 ± 0.01 μg Chl *a* L^{-1} at OSP. Small phytoplankton (< 5 μm) similarly decreased by > 3-fold along the transect, reaching highest concentrations of 1.87 ± 0.29 μg Chl *a* L^{-1} at P2 and gradually decreasing to 0.48 ± 0.02 μg Chl *a* L^{-1} at OSP. Based on size-fractionated Chl *a* measurements, larger phytoplankton comprised about half of the phytoplankton biomass at coastal stations

Fig. 2. Relative gene expression of (**A**) *P. granii METH*, (**B**) *G. cf. islandica METH*, and (**C**) *G. cf. islandica METE* under iron-replete (+Fe), iron-limited (−Fe) and iron-resupplied conditions in the presence (+B_{12}) or absence (−B_{12}) of vitamin B_{12}. All genes are normalized to actin (*ACT*) transcripts. Letters denote significant differences among treatments as determined through two-tailed homoscedastic *t*-tests ($p < 0.05$). Error bars represent ± 1 standard error associated with the mean [$n \geq 3$ except within the following treatments: *P. granii METH* +Fe/+B_{12}, −B_{12}/+Fe-resupply ($n = 2$); *P. granii METH* −Fe/−B_{12} ($n = 1$), *G. cf. islandica METE* −Fe/−B_{12} and −B_{12}/+Fe-resupply ($n = 2$)].

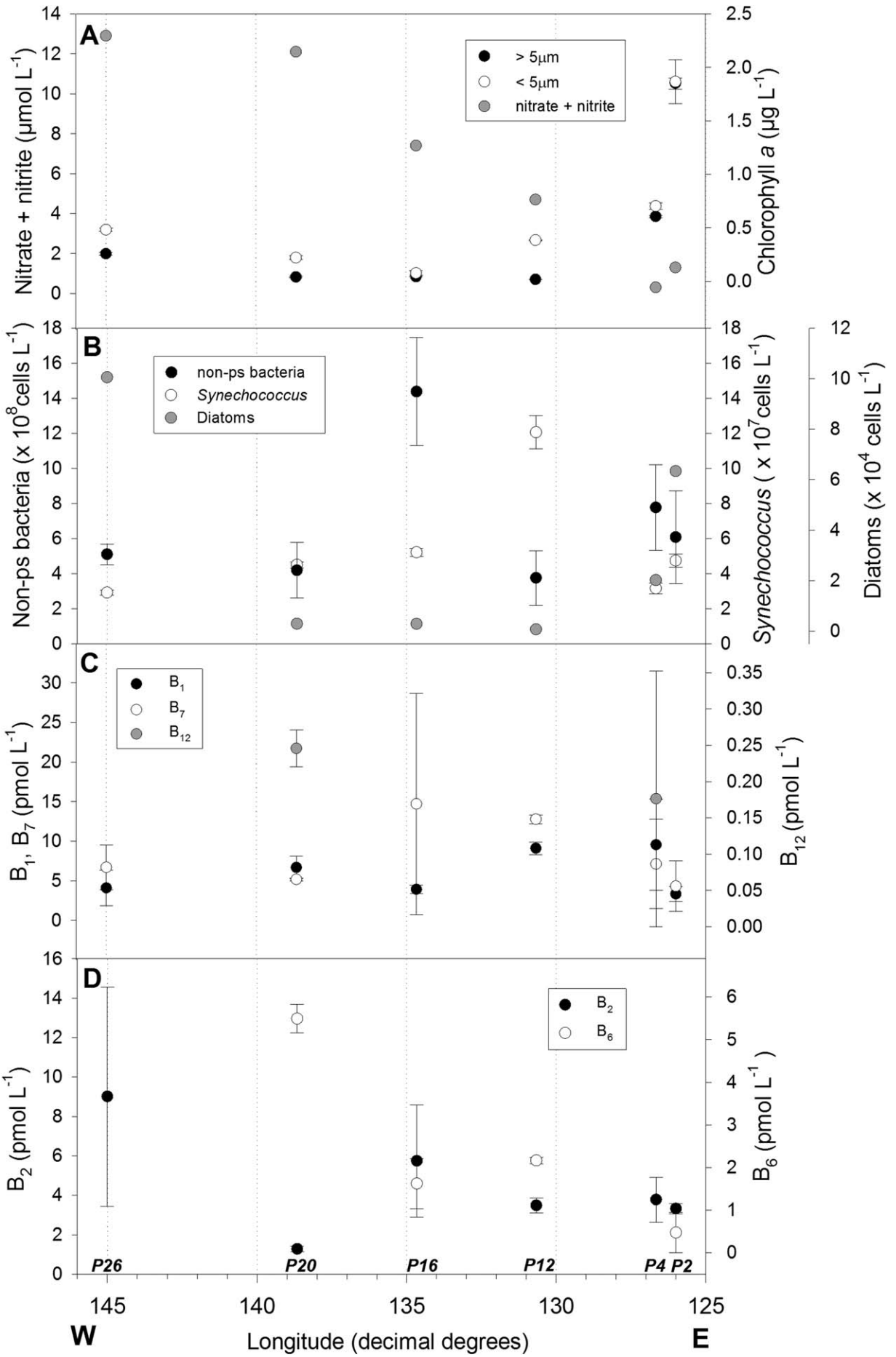
A
> 5μm
< 5μm
nitrate + nitrite
Nitrate + nitrite (μmol L-1)
Chlorophyll a (μg L-1)
B
non-ps bacteria
Synechococcus
Diatoms
Non-ps bacteria (x 10^8 cells L-1)
Synechococcus (x 10^7 cells L-1)
Diatoms (x 10^4 cells L-1)
C
B1
B7
B12
B1, B7 (pmol L-1)
B12 (pmol L-1)
D
B2
B6
B2 (pmol L-1)
B6 (pmol L-1)
P26
P20
P16
P12
P4
P2
145
140
135
130
125
W
Longitude (decimal degrees)
E

whereas small phytoplankton dominated at all other stations along the transect. Total chlorophyll concentrations were elevated at OSP relative to the adjacent station P20. This may have been associated with a recent iron deposition event within the vicinity of OSP near the time of sampling due to the eruption of Mt. Pavlof, a frequently active volcano within the Aleutian Range of the Alaskan Peninsula (*see* discussion for more details).

Diatom cell densities were highest at the coastal stations and substantially decreased along the Line-P transect, consistent with the declines in large phytoplankton Chl *a* concentrations (Fig. 3B). Diatom density was relatively high at P2 with 6.2×10^4 cells L^{-1}, decreased to 2×10^4 cells L^{-1} at P4, and remained below 3×10^3 cells L^{-1} at stations P12 through P20. Counts were elevated at OSP as compared to the preceding stations. The assemblage at the coastal stations was comprised mainly of centric diatoms, while the diatom population at OSP was mostly pennate diatoms, in particular, members of the genus *Pseudo-nitzschia*.

Neither cyanobacteria nor the non-photosynthetic (non-ps) bacteria cell counts followed any obvious spatial trends along the Line-P transect (Fig. 3B). Cyanobacteria counts were attributed to *Synechococcus*—cell densities fluctuated from approximately $3 \times 10^7 \pm 0.2 \times 10^7$ cells L^{-1} at OSP to $12 \times 10^7 \pm 0.9 \times 10^7$ cells L^{-1} at P12. Non-ps bacterial abundance was elevated at P16, with $14 \times 10^8 \pm 3 \times 10^8$ cells L^{-1}, while cell densities were comparatively lower at all other stations.

B-vitamin concentrations varied substantially along the Line-P transect (Fig. 3C,D). Vitamin B_1 (thiamine hydrochloride) concentrations ranged from 3.3 pmol L^{-1} to 9.5 pmol L^{-1}, with stations P4 and P12 having the highest concentrations. Vitamin B_7 (biotin) similarly fluctuated along the transect varying between 4.3 pmol L^{-1} and 14.7 pmol L^{-1}, with the highest concentration located at P16. Due to the large error associated between replicates and the SPE recovery reaching 180%, trace B_7 contamination from reagents used during preconcentration was possible. Vitamin B_2 (riboflavin) concentrations ranged from 1.3–9 pmol L^{-1} with the highest concentration at OSP. Vitamin B_6 (pyridoxal hydrochloride) ranged from 0.48 pmol L^{-1} to 5.49 pmol L^{-1} with a peak concentration at P20, and below the detection limit at stations at P4 and P26. The form of vitamin B_{12} measured, cyanocobalamin, fell below the limit of quantification (0.13 pmol L^{-1}) at all stations except P4 and P20, in which concentrations were 0.18 pmol L^{-1} and 0.25 pmol L^{-1}, respectively. B_1 and B_7 concentrations at OSP were on the lower end of those measured along the Line-P transect, while B_6 and B_{12} were below the detection limit.

Phytoplankton response to iron and vitamin enrichment experiments at OSP

Phytoplankton biomass increased during the incubation experiments in all treatments as indicated by Chl *a* within two size fractions (Fig. 4A). Initial Chl *a* concentrations were predominantly attributable to small phytoplankton (< 5 μm; 0.65 ± 0.25 μg Chl *a* L^{-1}) with large phytoplankton (> 5 μm) comprising approximately 24% of the biomass. The contribution of the large size fraction significantly increased following iron addition, reaching over 4 μg Chl *a* L^{-1} following 96 h of incubation ($p \leq 0.002$). Small phytoplankton biomass was approximately 4-fold lower than large phytoplankton in incubations receiving iron. $F_v : F_m$ assessment indicated iron limitation was alleviated following iron addition with a significant increase in ratios ($p < 0.001$; Fig. 4B). $F_v : F_m$ values of initial communities and treatments without iron ranged from 0.37 to 0.40, while treatments with iron achieved maximum values of 0.50–0.53.

Diatom populations in incubations with iron addition increased appreciably, reaching 40-fold higher densities (approximately 15×10^5 cells L^{-1}) compared to the initial diatom cell densities (4×10^4 cells L^{-1}; Fig. 4C). Total diatom abundance was the highest in the community receiving both iron and B_{12}, reaching 16×10^5 cells L^{-1}, and was the only treatment considered significantly different from initial diatom densities (T_0) and all incubations where iron was not added ($p < 0.03$). Diatom cell densities in treatments without iron also increased from those in the ambient seawater although concentrations were approximately 2-fold lower compared to the iron addition treatments. All incubations were dominated by *Pseudo-nitzschia* spp. Other diatom groups observed were comparatively less abundant across treatments and time points (Fig. 4C).

High-throughput sequencing of transcripts allowed for comparisons of relative community composition among the treatments. Consistent with light microscopy data, diatom transcripts increased from 8% of the eukaryotic plankton community to 20–28% in treatments without iron and 40–46% in treatments with iron added (Fig. 4D). Apart from diatoms and dictyochocophytes, all other major phytoplankton groups decreased in relative proportions compared to the initial community following incubation.

Fig. 3. (See previous page) Surface nitrate concentrations, phytoplankton biomass, cell densities, and dissolved concentrations for select vitamin forms along the Line-P transect. (**A**) Nitrate and nitrite concentrations and size-fractionated Chl *a*. (**B**) *Synechococcus*, non-photosynthetic (non-ps) bacteria and diatom cell densities. (**C**) Dissolved B_1, B_7, and B_{12} concentrations in surface seawater. (**D**) Dissolved B_2 and B_6 concentrations in surface seawater. The instrumental detection limit for each vitamin were as follows: 0.25 pmol L^{-1} for thiamine hydrochloride (B_1) and biotin (B_7), 0.13 pmol L^{-1} for riboflavin (B_2) and cyanocobalamin (B_{12}), and 0.38 pmol L^{-1} for pyridoxal hydrochloride (B_6). Error bars represent $\pm$ 1 standard error associated with the mean (for **A** and **B**, $n = 3$; for **C** and **D**, $n = 2$).

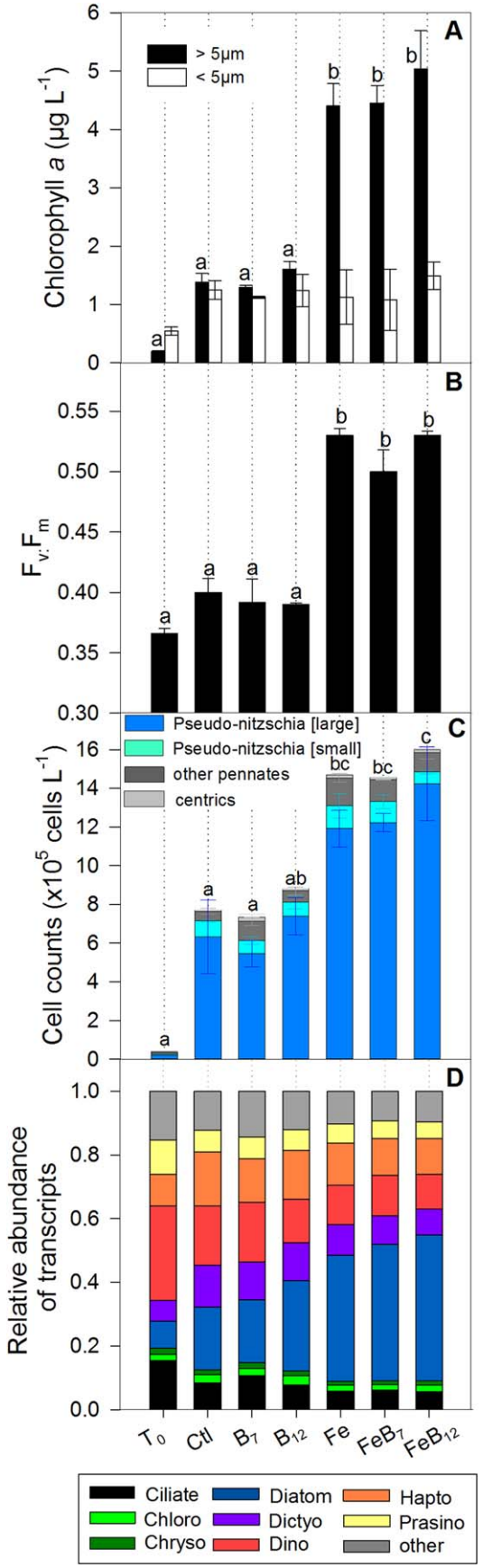

Metatranscriptomic community response to iron/vitamin additions

Key indicator genes encoding proteins involved in iron and vitamin metabolism were used to determine diatom community response to iron/vitamin enrichments (Fig. 5). Iron played a large role in driving expression changes, with B_7 and B_{12} additions alone having less of an impact on overall gene expression. In all iron-amended treatments, transcript abundance of the gene encoding the iron storage protein ferritin (*FTN*), involved in maintaining iron homeostasis in marine protists (Marchetti et al. 2009; Botebol et al. 2015; Pfaffen et al. 2015), increased at least 7-fold (Fig. 5A). Similarly, transcripts of fructose-bisphosphate aldolase class II (*class II FBA*), a metal-dependent aldolase involved in gluconeogenesis, glycolysis and the Calvin Cycle, increased approximately 8-fold as compared to the unamended control treatment (Horecker et al. 1972). *Class II FBA* transcripts have been previously demonstrated to be abundant under iron-replete conditions in diatoms and this protein is hypothesized to contain Fe^{2+} as a metal cofactor (Allen et al. 2012; Lommer et al. 2012). Transcripts corresponding to the iron starvation induced proteins 2A (*ISIP2A*), responsible for iron acquisition in diatoms (Morrissey et al. 2015), and *ISIP2B* decreased by approximately 3-fold and 73-fold, respectively, with very few transcripts associated with *ISIP2B* within iron addition treatments. Transcripts associated with fructose-bisphosphate aldolase class I (*class I FBA*), the metal-independent version of *class II FBA* found to be abundant under iron-limitation in diatoms (Allen et al. 2012; Lommer et al. 2012), similarly decreased by 8-fold after iron addition as compared to the control treatment. Expression levels of flavodoxin (*FLDA*), an iron-independent photosynthetic electron acceptor and proposed iron stress indicator gene in certain diatoms (Chappell et al. 2015), did not change within iron amended treatments compared to the control.

B_7 metabolism was also affected by iron addition, as *BIOB* transcripts increased 2-fold in treatments receiving iron compared to the unamended control treatment (Fig. 5B). However, two other genes involved in biotin metabolism, *BIOA* and *BIOF*, were not similarly overrepresented following iron

Fig. 4. Growth characteristics, diatom cell densities, and transcript abundances in iron and/or vitamin incubation experiments. (**A**) Size-fractionated Chl *a* concentrations, (**B**) Maximum photochemical yield of PSII ($F_v : F_m$), (**C**) Diatom cell counts obtained via light microscopy, and (**D**) Relative transcript abundance of eight major taxonomic groups in the initial seawater (T_0), unamended control (Ctl), B_7-only (B_7), B_{12}-only (B_{12}), iron-only (Fe), iron and B_7 (FeB_7), and iron and B_{12} (FeB_{12}) treatments following 96 h of incubation. For (**D**) Ciliate, ciliates; Chloro, chlorophytes; Chryso, chrysophytes; Diatom, diatoms; Dictyo, dictyochophytes; Dino, dinoflagellates; Hapto, haptophytes; Prasino, prasinophytes. Where present, error bars represent ± 1 standard error associated with the mean ($n \geq 2$). Letters denote significant differences among treatments as determined via one-way RM ANOVA and Holm-Sidak comparison tests ($p < 0.05$). For (**A**), only the >5 μm fraction was tested for significant differences among treatments.

addition. B_{12} status was assessed via transcript changes in the genes encoding METE and CBA1. Expression of both genes increased in treatments where iron was added without B_{12} (Fe and FeB_7). *CBA1* expression increased by approximately 2-fold compared to the control, while *METE* increased by 30-fold (Fig. 5). In contrast, transcripts corresponding to *METH* did not change in abundance within iron and/or vitamin amended treatments. The *METE* gene is present in some, but not all, diatoms with the gene being absent from sequenced transcriptomes of *Pseudo-nitzschia* species as well as the genome of *Pseudo-nitzschia multiseries* (Ellis et al. 2017). Thus, there was a clear distinction in the taxonomic assignment for *METE* in these diatom communities where transcripts were assigned to the raphid pennate diatom *Attheya septentrionalis* as opposed to most of the other diatom transcripts assigned to *Pseudo-nitzschia*, the dominant diatom genera following iron addition (Fig. 4C).

Pairwise comparison between the iron-amended and unamended control treatments revealed the differential expression of several other genes indirectly related to iron or vitamin metabolism, including nitrite reductase (*NIRB*), nitrate reductase (*NR*), 3-hydroxyacyl-acyl-carrier-protein (ACP) dehydratase (*FABZ*), and acetyl-coenzyme A (CoA) carboxylase (*ACACA*). Increased abundance of nitrogen assimilation transcripts *NR* and *NIRB* following iron addition likely allow previously iron-limited diatoms to take advantage of bioavailable iron in order to metabolize readily available nitrate from HNLC waters (Marchetti et al. 2012), while increases in *FABZ* and *ACACA* transcripts following iron addition may play a role in B_7 metabolism (*see* discussion).

Classifying genes based on their KO assignment and grouping them into module-level classifications enables a broader assessment of vitamin synthesis gene expression among treatments (Supporting Information Table 3). Transcript abundance within treatments receiving iron additions (Fe, FeB_7, FeB_{12}) responded similarly and clustered together (Fig. 6). All B-vitamin modules were enriched to varying degrees following iron addition as compared to the unamended control or vitamin-only treatments. A putative B_{12} synthesis/repair/salvage module in diatoms was elevated by 2-fold within the Fe and FeB_7 treatments as compared to the control, with FeB_{12}, B_{12}, and B_7 treatments also demonstrating elevated expression as compared to the control, though to a lesser extent. The methionine synthesis module (which contains the *METH* and *METE* genes) followed a similar pattern to the B_{12} module, with enrichment of 1.5- and 1.3-fold in the Fe and FeB_7 treatments, respectively, largely driven by changes in *METE* transcript abundance (Supporting Information Table 3). The B_7 synthesis module was elevated 2-fold after iron addition, with enrichment also apparent in the B_7 and B_{12} treatments but to a lesser extent. Both vitamin B_6 and B_2 modules were enriched by approximately 1.6- and 1.4-fold, respectively, within all three iron-amended treatments, while the B_1 module increased 1.5-fold in the FeB_7 treatment but was only slightly increased in the Fe and FeB_{12} treatments.

Discussion

Line-P transect and vitamin dynamics

During the June 2013 cruise, we observed higher than typical Chl *a* concentrations at OSP (0.75 μg L^{-1} Chl *a*; Fig. 4A), which generally supports lower phytoplankton biomass (0.3–0.5 μg L^{-1} Chl *a*; Harrison et al. 2004). In May of 2013, one of Alaska's most active volcanoes, Mt. Pavlof, began erupting and released ash up to 22,000 feet above sea level. NOAA HYSPLIT (Hybrid Single-Particle Lagrangian Integrated Trajectory model; Stein et al. 2015) particle trajectories estimated that the ash cloud may have reached OSP by late May. Based on these observations, we suspect the OSP phytoplankton community was exposed to a higher than usual amount of iron input in the form of volcanic ash deposition due to the eruption, resulting in relatively high Chl *a* concentrations when compared to adjacent Line-P stations and the historical average. Regardless, our iron-amended treatments indicated increases in Chl *a*, $F_v : F_m$, and diatom cell counts as compared to the unamended control treatment, suggesting that the ambient phytoplankton community at OSP was still iron-limited (Fig. 4A–D).

Our Line-P transect analysis began at coastal station P2 and ended at OSP, following expected trends of increasing nitrate and decreasing phytoplankton biomass and diatom abundance (with the exception of OSP as previously discussed). This is consistent with the transition from coastal to HNLC waters occurring along the transect, where surface dissolved iron concentrations at P4 are typically > 0.1 nmol L^{-1}, and decrease westward to approximately < 0.05 nmol L^{-1} at OSP (Harrison et al. 2004). However, select forms of B-vitamins measured and bacteria densities did not follow any obvious onshore-offshore trends. Localized peaks in *Synechococcus* cell densities occurred at the transition station P12, and in non-ps bacteria cell densities at P16, but these hotspots of bacterial biomass did not strongly co-vary with either diatom abundance, vitamin concentrations, or Chl *a* concentrations (Fig. 3). Alternatively, it is possible that non-ps bacterial growth was primarily influenced by organic matter availability, which was not measured in this study. Grazing by microzooplankton, which was also not measured, may have additionally influenced both non-ps and *Synechococcus* abundances (Zöllner et al. 2009). Additionally, these vitamin measurements represent only a fraction of the total dissolved vitamin pool, and multiple forms exist in varying abundances and importance in the marine environment (Helliwell et al. 2016; Heal et al. 2017). Therefore, quantification of remaining vitamin fractions are necessary in order to gain a comprehensive understanding of the relationships between macro- and micro-nutrients, bacterial and phytoplankton biomass, and dissolved vitamins along the Line-P

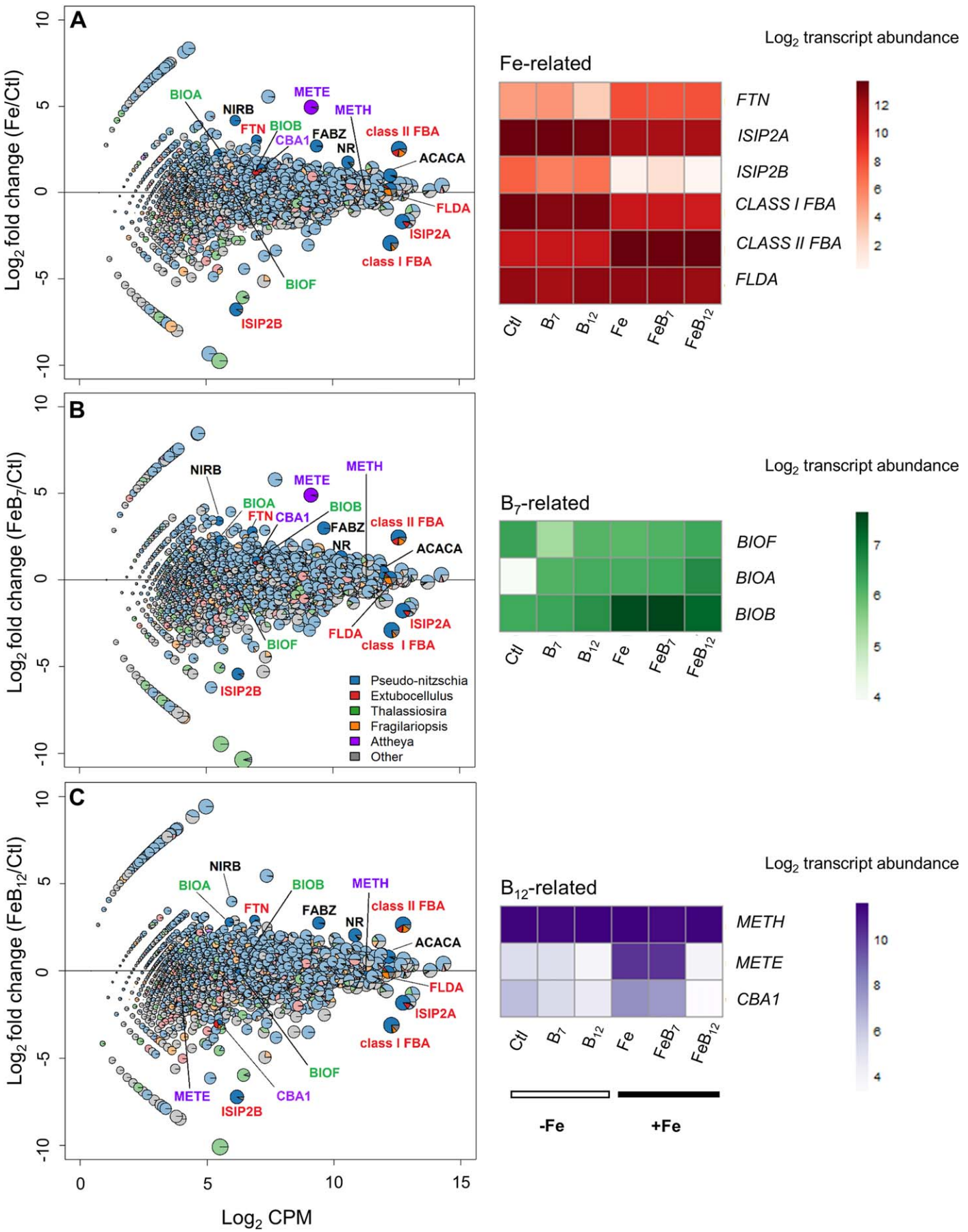
A
B
C
Log2 fold change (Fe/Ctl)
Log2 fold change (FeB7/Ctl)
Log2 fold change (FeB12/Ctl)
Log2 CPM
BIOA
NIRB
METE
METH
FTN
BIOB
CBA1
FABZ
NR
class II FBA
ACACA
FLDA
ISIP2A
class I FBA
BIOF
ISIP2B
Pseudo-nitzschia
Extubocellulus
Thalassiosira
Fragilariopsis
Attheya
Other
Log2 transcript abundance
Fe-related
FTN
ISIP2A
ISIP2B
CLASS I FBA
CLASS II FBA
FLDA
B7-related
BIOF
BIOA
BIOB
B12-related
METH
METE
CBA1
Ctl
B7
B12
Fe
FeB7
FeB12
-Fe
+Fe

transect. However, the measured dissolved vitamin concentrations reported here are useful in defining ranges in concentrations along the transect in comparison to other regions of the coastal Pacific Ocean in which vitamin quantification has been performed in a consistent manner (Sañudo-Wilhelmy et al. 2012).

B_{12} (cyanocobalamin) was detected in the highest concentration at station P20 (0.25 ± 0.03 pmol L^{-1}) and was below the detection limit of 0.13 pmol L^{-1} at all other locations apart from P4, where variability among replicates was high. This is in contrast to the cyanocobalamin concentrations obtained within the California Current System (CCS), which ranged from below detection to as high as 15 pmol L^{-1} in surface waters (Sañudo-Wilhelmy et al. 2012). These comparatively lower cyanocobalamin concentrations alone however do not indicate B_{12} limitation of the ambient phytoplankton community in the NE Pacific Ocean. The other forms of B_{12} not measured in this study, including the other cobalamin upper-ligand variants and all variants of pseudocobalamin, could have been more abundant than cyanocobalamin in these waters. Given that in a number of cobalamin and pseudocobalamin producers the cyano-upper ligand has not been detected but all others have, these other variants may be more important in fueling growth of B_{12}-dependent microorganisms (Heal et al. 2017).

Although evidence of widespread B_{12} limitation was not observed through our Chl *a* measurements within the incubation experiments (i.e., treatments with B_{12} addition did not achieve significantly higher Chl *a* vs. non-B_{12} treatments), the FeB_{12} treatment was the only incubation to achieve diatom cell densities significantly higher than all of the non-iron containing treatments. Furthermore, our transcriptomic findings indicate that there is potential for species-specific B_{12} limitation in phytoplankton with obligate B_{12} requirements following alleviation of iron limitation (*see* further discussion below). We interpret this to suggest that since iron was the primary limiting nutrient, B_{12} enrichment alone could not result in increased growth. However, the combination of iron and B_{12} resulted in the highest diatom abundances observed, and given the transcriptomic response of certain diatom community members following iron addition, we speculate differences in phytoplankton biomass between the FeB_{12} treatment and those in which iron and B_{12} were added independently might have occurred with a longer incubation time.

Interestingly, B_6 (pyridoxal hydrochloride) concentrations reached a maximum of 5.49 ± 0.33 pmol L^{-1} at station P20 and were below detection at P4 and OSP. These concentrations were considerably lower than the maximum of 200 pmol L^{-1} observed within the CCS surface waters (Sañudo-Wilhelmy et al. 2012). B_6 requirements in phytoplankton are not well defined, although the stark contrast in vitamin concentrations between the coastal and open ocean environments suggests pronounced differences in production and/or consumption of this vitamin possibly due to differences in community composition of bacteria, phytoplankton, or both.

Vitamin synthesis in diatoms

During our incubation experiments at OSP, B-vitamin genes encompassed within KEGG biosynthesis and synthesis/repair/salvage vitamin pathways were overrepresented in phytoplankton communities receiving iron additions as compared to the unamended control (Fig. 6). These results suggest that initially iron-limited diatom communities do not produce as many vitamins due to either having reduced demand while growing at a slower rate, or not having the iron necessary to fuel iron-dependent vitamin synthesis. The increase in vitamin transcript abundance following iron addition likely represents a combination of the increased vitamin production required to fuel elevated rates of metabolic activity and relief of iron stress on vitamin biosynthesis.

Three of the four genes involved in biotin B_7 biosynthesis were identified in our metatranscriptomes, with the B_7 biosynthesis module increasing 2-fold in expression after iron addition. Although this study provides strong support for B_7 biosynthesis in *Pseudo-nitzschia*, it remains unclear how this genus and others are producing the precursor to B_7, dethiobiotin, given the absence of a *BIOD* ortholog (Croft et al. 2006). The gene *BIO3-BIO1*, which encodes for a bifunctional fusion protein with the functionality of both *BIOD* (*BIO3*) and *BIOA* (*BIO1*), may be a likely candidate (Muralla et al. 2008). This gene has been previously identified in the *P. tricornutum* genome (Bowler et al. 2008) and is also present in our metatranscriptome sequences, albeit with very low transcript abundance and only present in the iron-enriched

Fig. 5. (See previous page) Diatom-specific gene expression responses to iron and/or vitamin additions. (**A**) Fe vs. control (Ctl), (**B**) FeB_7 vs. Ctl, and (**C**) FeB_{12} vs. Ctl. The y-axis corresponds to the $\log_2$ fold change ratio of normalized transcripts between the two treatments, while the x-axis represents the $\log_2$ CPM, or average transcript abundance. Each pie represents transcripts associated with a single gene (KEGG KO or gene definition, *see* methods). Pies increase in size with increasing CPM and absolute value of the fold change. Pies are colored by distribution of transcripts from each of the four most abundant diatom genera as well as the diatom genus *Attheya*. In each graph, genes with transcripts within only one of the treatments are displayed on arms to the left. Iron and vitamin-related genes, along with a few other genes of interest are labeled: iron-related (red): *FTN*, ferritin; *ISIP2A*, iron-starvation induced protein A; *ISIP2B*, iron-starvation induced protein B; *FLDA*, flavodoxin I; *class I FBA*, fructose-bisphosphate aldolase class I; *class II FBA*, fructose-bisphosphate aldolase class II. B_7-related proteins (green): *BIOB*, biotin synthase; *BIOA*, DAPA synthase; *BIOF*, KAPA synthase. B_{12}-related proteins (purple): *METH*, B_{12}-dependent methionine synthase; *METE*, B_{12}-independent methionine synthase; *CBA1*, cobalamin acquisition protein 1. Other proteins indirectly related to iron and/or vitamins (black): *FABZ*, 3-hydroxyacyl-acp dehydratase; *ACACA*, acetyl-coenzyme A; *NR*, nitrate reductase; *NIRB*, nitrite reductase. Pies corresponding to genes not mentioned in the text are lightly shaded. Displayed in adjacent heatmaps are the $\log_2$ normalized transcript abundances of genes of interest partitioned into iron/vitamin categories within all treatments.

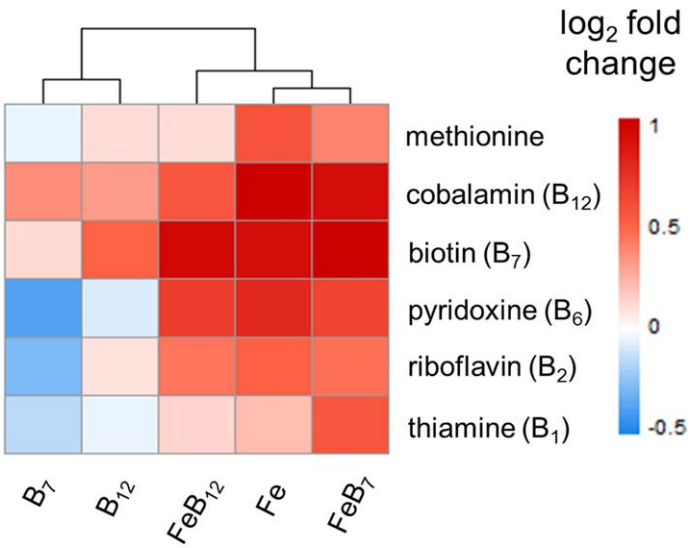

Fig. 6. Module-level expression responses of biosynthetic vitamin pathways in diatoms. Diatom normalized read counts contained within each KEGG vitamin synthesis module were summed within a treatment and expressed as the $\log_2$ fold change compared to the unamended control treatment. Genes contained within each vitamin module and the associated contigs with the most reads mapped are provided in Supporting Information Table 3. The dendrogram reflects similarity in expression responses among treatments and was created using Euclidean distance and hierarchical clustering.

treatments. In addition, the majority of *BIO3-BIO1* transcripts belong to the genus *Chaetoceros*, which was not an abundant taxon in the incubations, while the majority of transcripts for all other B_7 biosynthesis genes (*BIOF*, *BIOA*, *BIOB*) were taxonomically associated to *Pseudo-nitzschia*. It remains unclear whether *Pseudo-nitzschia* may additionally utilize *BIO3-BIO1* or instead rely on an unidentified enzyme to synthesize dethiobiotin.

Based on the presence of vitamin transcripts for genes involved in vitamin synthesis within our metatranscriptomes, diatoms at OSP are likely able to produce vitamins B_2 and B_7. However, only incomplete pathways for vitamins B_1, B_6, and B_{12} were identified. This may suggest that diatoms are either auxotrophs for these latter vitamins, that they possess the ability to process intermediates in order to relieve auxotrophy, vitamin-independent metabolic alternative pathways are invoked (e.g., *METE*), or that transcripts were were missed by our methods. As it is possible that transcriptome sequencing depth did not capture the presence of the full biosynthetic pathways associated with vitamin B_1 or B_6 production, it should not be assumed that diatoms present within the incubations are truly missing key components of certain vitamin synthesis pathways.

Unexpectedly, transcripts for genes encoding eight out of approximately 21 biosynthetic enzymes involved in the production of B_{12} were identified within diatoms, mainly assigned to the genus *Pseudo-nitzschia*. These include genes within the KEGG final synthesis/repair/salvage module and two additional synthesis genes responsible for production of intermediates that are not included in the KEGG module (Warren et al. 2002; Supporting Information Fig. 4). All but two of these eight genes (*COBB*, cobyrinic acid a,c-diamide synthase, and *COBA*, cob(I)alamin adenosyltransferase; the only two genes with the majority of transcripts associated with genera other than *Pseudo-nitzschia*) were also identified in the genome of *Pseudo-nitzschia multiseries* (JGI Genome Portal; Supporting Information Table 3). Module expression was elevated by 2-fold in the Fe and FeB_7 treatments compared to the unamended control, with a comparatively reduced response in the FeB_{12} treatment. It is unlikely that diatoms possess the ability to synthesize B_{12} de novo since the full biosynthetic pathway has not yet been identified in any eukaryote (Warren et al. 2002). However, the pattern of increased transcript abundance of genes involved in B_{12} synthesis/repair/salvage in diatoms under conditions consistent with B_{12} stress and/or limitation suggests diatoms may have some capacity to process B_{12} intermediates.

Although bacterial contamination during eukaryotic-targeted sequencing is possible, sequence homology analyses indicated all environmental *COB* genes found in the metatranscriptomes presented here closely match unannotated genes within genomes and transcriptomes of diatoms, green algae, cryptophytes and other protists available within GenBank's non-redundant and MMETSP protein databases (e-value < 0.001). Additionally, these environmental *COB* contigs contained conserved domain regions diagnostic of each *COB* protein, verifying their role within B_{12} synthesis. We therefore argue against bacterial contamination resulting in the presence of these genes in our metatranscriptomes or non-specific functional assignments for the contigs identified in diatoms. Instead we speculate *COB* presence within marine eukaryotes is widespread. *COB*-like genes have been observed in eukaryotes previously, particularly in diatoms, dinoflagellates and haptophytes (Helliwell et al. 2011; Bertrand et al. 2012; Zhang et al. 2013; Helliwell et al. 2016). Furthermore, recent evidence suggests divergent lineages of phytoplankton are capable of chemically modifying the lower axial ligand of the B_{12} molecule by incorporating 5, 6-di- methylbenzimidazole (DMB) acquired exogenously from growth medium (Helliwell et al. 2016), and thereby converting a form unable to support maximum growth (pseudocobalamin) to one that can (cobalamin). The genes encoding proteins thought to be involved in the remodeling process include *COBT*, *COBC*, and *COBS*, identified within the genome of *Chlamydomonas reinhardtii* and transcriptome of *Pavlova lutheri*, both of which exhibit remodeling in culture (Supporting Information Fig. 4; Anderson et al. 2008; Helliwell et al. 2016). *COBT* and *COBS* were identified in the diatom metatranscriptomes presented here, with increased transcripts following iron enrichment (Supporting Information Fig. 4; Supporting Information Table 3), suggesting marine diatoms in the NE

Pacific Ocean may be utilizing these genes for remodeling purposes. Further studies are necessary to determine whether pseudocobalamin in our study region is bioavailable and whether members of the diatom community are able to modify it in order to fulfill their vitamin requirements, as has been demonstrated in laboratory cultures (Helliwell et al. 2016; Heal et al. 2017).

Implications of iron status on B_7 production by diatoms

We demonstrate here for the first time that *BIOB* expression and presumably B_7 production in *P. granii* is reduced under iron-limiting growth conditions. This was further supported by the laboratory iron resupply experiments, in which previously iron-limited *P. granii* cells increased *BIOB* expression following the addition of iron. Similar to our laboratory experiments, iron-limited natural diatom communities increased transcript abundance of *BIOB* following iron addition at OSP. The implications of being in a growth-limited state must be taken into consideration when comparing gene expression across treatments (Bremer and Dennis, 1996). In our laboratory experiments, reductions in growth rate alone did not control *BIOB* expression, as light-limited *P. granii* cells exhibited expression levels consistent with replete cultures. This suggests that *BIOB* expression is directly regulated by iron status and is in agreement with previous studies reporting that iron limitation can trigger a transcriptional change in iron-dependent genes within *P. granii* and effectively induce an alternative gene repertoire (Marchetti et al. 2012). A reduction in B_7 biosynthesis may thus be an additional strategy used to conserve iron within iron-limited diatoms.

In addition to the three genes directly involved in B_7 biosynthesis, other B_7-related genes were identified and found to be affected by iron addition at OSP. One abundant gene, 3-hydroxyacyl-ACP dehydratase (*FABZ*), was overrepresented by approximately 7-fold in all iron-amended treatments as compared to the control. FABZ is a component of fatty acid synthesis, a pathway linked to B_7 biosynthesis due to its role in producing the precursor pimeloyl-ACP methyl ester, used by BIOH to initiate biotin production (Lin et al. 2010). Similarly, acetyl-CoA carboxylase (*ACACA*), encoding a biotin-dependent enzyme that catalyzes the transfer of carboxyl groups critical during fatty acid synthesis (also known as biotin carboxylase) was overrepresented following iron addition by 1.7-fold. Although expression patterns indicate iron-enriched diatoms increase expression of *ACACA*, this trend is not necessarily due to iron as previous studies report *ACACA* transcript abundance is a direct function of cellular growth rate (Li and Cronan 1993). Increased *BIOB* following iron addition, perhaps in conjunction with FABZ, may lead to elevated B_7 production by rapidly blooming diatoms and subsequently result in increased B_7 availability to auxotrophs within their surrounding environment.

There are multiple possibilities for how iron-limited marine diatoms may be compensating for decreased B_7 biosynthetic production. Intracellular B_7 quotas could decrease to allow cells to persist with less B_7, similar to acclimated diatoms under iron limitation decreasing cellular iron quotas (Harrison and Morel 1986). Alternatively, cells may switch modes of B_7 metabolism from production to uptake when iron is in limited supply. Although, to our knowledge, B_7 uptake by diatoms capable of producing the vitamin has not yet been observed, *Pseudo-nitzschia pungens* has been found to be auxotrophic for B_7 (Tang et al. 2010). An uptake mechanism therefore must exist in diatoms and may be present in B_7-producing diatoms as well. Interestingly, the yeast *S. cerevisiae* decreases B_7 biosynthesis under iron limitation and activates the acquisition of external B_7 through the proton-dependent permease vitamin-H transporter 1 (VHT1) (Shakoury-Elizeh et al. 2004). This allows intracellular iron to be allocated to crucial iron-dependent metabolic pathways, reducing overall cellular iron demand, while still maintaining an adequate supply of B_7 for continued growth. A similar response to iron limitation may also occur in *P. granii*, which under iron-limited conditions, has higher *BIOB* transcript abundance when B_7 is absent as compared to when B_7 is present. This pattern in gene expression may suggest an ability to take up B_7 from their external environment. Such a response was not observed within our iron addition experiments in the Northeast Pacific Ocean, with *BIOB* expression levels remaining constant under iron-limiting conditions with or without B_7 addition. This is likely due to there being sufficient B_7 concentrations at OSP (6.7 ± 2.8 pmol L^{-1}), resulting in similar B_7 dynamics between the B_7 treatment and the unamended control.

Implications of iron status on B_{12} utilization by diatoms

Laboratory studies presented here with *Grammonema cf. islandica* under varying iron/B_{12} conditions demonstrate *METE* gene expression is primarily regulated by B_{12} status with minimal to no influence of iron status (Fig. 2C). Therefore, we must interpret the 30-fold increase in transcript abundance of *METE* we observed in natural diatom assemblages following iron addition to be due to B_{12} concentrations becoming limiting for iron-stimulated diatoms. Insufficient acquisition from their environment would have caused *METE*-possessing diatoms to begin producing the B_{12}-independent form of methionine synthase (Fig. 5). In addition, *CBA1*, another gene demonstrated to increase under B_{12} limitation (Bertrand et al. 2012), increased 3-fold in treatments where iron was added without vitamin B_{12}. The community was furthermore relieved of B_{12} limitation when B_{12} was added in conjunction with iron; both *METE* and *CBA1* transcripts decreased in the FeB_{12} treatment as compared to the unamended control (by 2.5- and 8.2-fold, respectively). Taken together, we conclude that the subarctic NE Pacific Ocean diatom community we examined was driven into B_{12} limitation following iron addition. The emergence of increased expression in B_{12}-sensitive indicator genes following iron addition co-occurs with surface dissolved cyanocobalamin

concentrations below 0.13 pmol L^{-1} at OSP (Fig. 3C). Because *METE* and *CBA1* were not abundant in the unamended control or ambient seawater, sufficient concentrations of B_{12} were likely present to support growth of iron-limited cells but were quickly depleted as the *Pseudo-nitzschia*-dominated bloom progressed. As all examined transcriptomes of *Pseudo-nitzschia* species lack *METE* (Ellis et al. 2017), the iron-stimulated *Pseudo-nitzschia* bloom may have consumed and outpaced the B_{12} supply. These conditions allowed for a diatom containing *METE* that was not initially abundant in the community, most likely belonging to, or closely-related to the genus *Attheya*, to increase their abundance of *METE* transcripts (Fig. 5A,B).

This work serves as compelling support for iron-induced vitamin B_{12} limitation in the Northeast Pacific Ocean. Several studies have demonstrated that low concentrations of vitamins can control phytoplankton biomass, with communities stimulated following vitamin enrichment experiments (Sañudo-Wilhelmy et al. 2006; Gobler et al. 2007; Bertrand et al. 2012; Koch et al, 2012; Bertrand et al. 2015). In such experiments, addition of B_1 and B_{12} resulted in community composition shifts (Gobler et al. 2007, Koch et al. 2012). Although in our study there were no obvious differences in phytoplankton biomass as a result of B_{12} enrichment, either with or without iron, we hypothesize shifts in community composition may have occurred if more time had elapsed, as perceived from the molecular indications of B_{12} limitation following iron addition within certain members of the diatom community by the end of our experiments.

Conclusions

Given the results of this study, it is probable that iron limitation reduces the amount of diatom-produced vitamin B_7 available to other auxotrophic microorganisms. The consequences would be most profound in regions where diatoms are a major supplier. Under iron-limiting conditions, auxotrophic microbes may then be forced to compete for a scarce resource as iron-limited diatoms reduce B_7 production and possibly transition to taking up vitamins from their environment. Conversely, following ephemeral iron enrichment events such as those observed during our field study with the eruption of Mt. Pavlof, increased demands for vitamin B_{12} may result in surface water depletion and subsequent community composition shifts. In our study, the emergence of *METE*-containing diatoms along with the increased expression of *METE* following iron enrichment provided evidence for B_{12} limitation in at least some members of the diatom community. Furthermore, we report that iron-limited diatoms produce fewer vitamin synthesis transcripts (for B_1, B_2, B_6, B_7, and B_{12}) as compared to cells enriched with iron, suggesting they either require less vitamins when growing more slowly, or they may lack the essential resources necessary to fuel their production.

References

Agusti, S., J. Gonzalez-Gordillo, D. Vaque, M. Estrada, M. I. Cerezo, G. Salazar, J. M. Gasol, and C. M. Duarte. 2015. Ubiquitous healthy diatoms in the deep sea confirm deep carbon injection by the biological pump. Nat. Commun. **6**: 1–8. doi:10.1038/ncomms8608

Alexander, H., B. D. Jenkins, T. A. Rynearson, M. A. Saito, M. L. Mercier, and S. T. Dyhrman. 2012. Identifying reference genes with stable expression from high throughput sequence data. Front. Microbiol. **3**: 385. doi:10.3389/fmicb.2012.00385

Allen, A. E., A. Moustafa, A. Montsant, A. Eckert, P. G. Kroth, and C. Bowler. 2012. Evolution and functional diversification of fructose bisphosphate aldolase genes in photosynthetic marine diatoms. Mol. Biol. Evol. **29**: 367–379. doi:10.1093/molbev/msr223

Altschul, S. F., W. Gish, W. Miller, E. W. Myers, and D. J. Lipman. 1990. Basic local alignment search tool. J. Mol. Biol. **215**: 403–410. doi:10.1016/S0022-2836(05)80360-2

Anderson, P. J., J. Lango, C. Carkeet, A. Britten, B. Kra, B. D. Hammock, and J. R. Roth. 2008. One pathway can incorporate either adenine or dimethylbenzimidazole as an alpha-axial ligand of B12 cofactors in Salmonella enterica. J. Bacteriol. **190**: 1160–1171. doi:10.1128/JB.01386-07

Armbrust, E. V. 2009. The life of diatoms in the world's oceans. Nature **459**: 185–192. doi:10.1038/nature08057

Behrenfeld, M. J., E. Boss, D. A. Siegel, and D. M. Shea. 2005. Carbon-based ocean productivity and phytoplankton physiology from space. Global Biogeochem. Cycles **19**: 1–14. doi:10.1029/2004GB002299

Behrenfeld, M. J., and A. J. Milligan. 2013. Photophysiological expressions of iron stress in phytoplankton. Annu. Rev. Mar. Sci. **5**: 217–246. doi:10.1146/annurev-marine-121211-172356

Bertrand, E. M., M. A. Saito, J. M. Rose, C. R. Riesselman, M. C. Lohan, A. E. Noble, P. A. Lee, and G. R. DiTullio. 2007. Vitamin B12 and iron colimitation of phytoplankton growth in the Ross Sea. Limnol. Oceanogr. **52**: 1079–1093. doi:10.4319/lo.2007.52.3.1079

Bertrand, E. M., M. A. Saito, P. A. Lee, R. B. Dunbar, P. N. Sedwick, and G. R. Ditullio. 2011. Iron limitation of a springtime bacterial and phytoplankton community in the Ross Sea: Implications for vitamin B12 nutrition. Front. Microbiol. **2**: 1–12. doi:10.3389/fmicb.2011.00160

Bertrand, E. M., A. E. Allen, C. L. Dupont, T. M. Norden-Krichmar, J. Bai, and R. E. Valas. 2012. Influence of cobalamin scarcity on diatom molecular physiology and identification of a cobalamin acquisition protein. Proc. Natl. Acad. Sci. USA. **109**: 1762–1771. doi:10.1073/pnas.1201731109

Bertrand, E. M., and others. 2015. Phytoplankton-bacterial interactions mediate micronutrient colimitation at the coastal Antarctic sea ice edge. Proc. Natl. Acad. Sci. USA. **112**: 9938–9943. doi:10.1073/pnas.1501615112

Birol, I., and others. 2009. De novo transcriptome assembly with ABySS. Bioinformatics **25**: 2872–2877. doi:10.1093/bioinformatics/btp367

Bolger, A. M., M. Lohse, and B. Usadel. 2014. Trimmomatic: A flexible trimmer for Illumina sequence data. Bioinformatics **30**: 2114–2120. doi:10.1093/bioinformatics/btu170

Botebol, H., and others. 2015. Central role for ferritin in the day/night regulation of iron homeostasis in marine phytoplankton. Proc. Natl. Acad. Sci. USA. **112**: 1–6. doi:10.1073/pnas.1506074112

Bowler, C., and others. 2008. The Phaeodactylum genome reveals the evolutionary history of diatom genomes. Nature **456**: 239–244. doi:10.1038/nature07410

Boyd, P. W., and others. 2007. Mesoscale iron enrichment experiments 1993 – 2005: Synthesis and future directions. Science **315**: 612–618. doi:10.1126/science.1131669

Brand, L. E., R. R. L. Guillard, and L. S. Murphy. 1981. A method for the rapid and precise determination of acclimated phytoplankton reproduction rates. J. Plankt. Res. **3**: 193–201.

Bremer, H., and P. P. Dennis. 1996. Modulation of chemical composition and other parameters of the cell by growth rate, p. 1553–1569. *In* F. C. Neidhardt, and others. [eds.], Escherichia coli and Salmonella typhimurium: Cellular and molecular biology. American Society for Microbiology. Escherichia coli and Salmonella: cellular and molecular biology, 2nd ed., vol. 2. American Society for Microbiology Press, Washington, D.C.

Chappell, P. D., L. P. Whitney, J. R. Wallace, A. I. Darer, S. Jean-Charles, and B. D. Jenkins. 2015. Genetic indicators of iron limitation in wild populations of Thalassiosira oceanica from the northeast Pacific Ocean. ISME J. **9**: 592–602. doi:10.1038/ismej.2014.171

Croft, M. T., A. D. Lawrence, E. Raux-Deery, M. J. Warren, and A. G. Smith. 2005. Algae acquire vitamin B_{12} through a symbiotic relationship with bacteria. Nature **438**: 90–93. doi:10.1038/nature04056

Croft, M. T., M. J. Warren, and A. G. Smith. 2006. Algae need their vitamins. Eukaryot. Cell **5**: 1175–1183. doi:10.1128/EC.00097-06

de Baar, H. J. W., and others. 2005. Synthesis of iron fertilization experiments: From the iron age in the age of enlightenment. J. Geophys. Res. Oceans **110**: 1–24. doi:10.1029/2004JC002601

Ellis, K. A., N. R. Cohen, C. Moreno, and A. Marchetti. 2017. Cobalamin-independent methionine synthase distribution and influence on vitamin B12 growth requirements in marine diatoms. Protist **168**: 32–47. doi:10.1016/j.protis.2016.10.007

Gobler, C. J., C. Norman, C. Panzeca, G. T. Taylor, and S. A. Sañudo-Wilhelmy. 2007. Effect of B-vitamins (B1, B12) and inorganic nutrients on algal bloom dynamics in a coastal ecosystem. Aquat. Microb. Ecol. **49**: 181–194. doi:10.3354/ame01132

Gorbunov, M. Y., and P. G. Falkowski. 2005. Fluorescence induction and relaxation (FIRe) technique and instrumentation for monitoring photosynthetic processes and primary production in aquatic ecosystems, p. 1029–1031. *In* A. van der Est and D. Bruce [eds.], Photosynthesis: Fundamental aspects to global perspectives. Allen Press.

Harrison, G. I., and F. M. M. Morel. 1986. Response of the marine diatom Thalassiosira weissflogii to iron stress. Limnol. Oceanogr. **31**: 989–997. doi:10.4319/lo.1986.31.5.0989

Harrison, P. J., F. A. Whitney, A. Tsuda, H. Saito, and K. Tadokoro. 2004. Nutrient and plankton dynamics in the NE and NW Gyres of the subarctic Pacific Ocean. J. Oceanogr. **60**: 93–117. doi:10.1023/B:JOCE.0000038321.57391.2a

Heal, K. R., L. T. Carlson, A. H. Devol, E. V. Armbrust, J. W. Moffett, D. A. Stahl, and A. E. Ingalls. 2014. Determination of four forms of vitamin B 12 and other B vitamins in seawater by liquid chromatography/tandem mass spectrometry. Rapid Commun. Mass Spectrom. **18**:2398–2404. doi:10.1002/rcm.7040

Heal, K. R., and others. 2017. Two distinct pools of B12 analogs reveal community interdependencies in the ocean. Proc. Natl. Acad. Sci. USA. **114**: 364–369. doi:10.1073/pnas.1608462114

Helliwell, K. E., G. L. Wheeler, K. C. Leptos, R. E. Goldstein, and A. G. Smith. 2011. Insights into the evolution of vitamin B 12 auxotrophy from sequenced algal genomes. Mol. Biol. Evol. **28**: 2921–2933. doi:10.1093/molbev/msr124

Helliwell, K. E., and others. 2016. Cyanobacteria and eukaryotic algae use different chemical variants of vitamin B12. Curr. Biol. **8**: 999–1008. doi:10.1016/j.cub.2016.02.041

Horecker, B. L., O. Tsolas, and C. Y. Lai. 1972. Enzym. **7**: 213–258. doi:10.1016/S1874-6047(08)60450-3

Jarrett, J. T. 2005. The novel structure and chemistry of iron–sulfur clusters in the adenosylmethionine-dependent radical enzyme biotin synthase. Arch. Biochem. Biophys. **433**: 312–321. doi:10.1016/j.abb.2004.10.003

Johnson, Z. I., R. Shyam, A. E. Ritchie, C. Mioni, V. P. Lance, J. W. Murray, and E. R. Zinser. 2010. The effect of iron- and light-limitation on phytoplankton communities of deep chlorophyll maxima of the western Pacific Ocean. J. Mar. Res. **68**: 283–308. doi:10.1357/002224010793721433

Keeling, P. J., and others. 2014. The marine microbial eukaryote transcriptome sequencing project (MMETSP): Illuminating the functional diversity of eukaryotic life in the oceans through transcriptome sequencing. PLoS Biol. **12**: e1001889. doi:10.1371/journal.pbio.1001889

King, A. L., S. A. Sañudo-Wilhelmy, K. Leblanc, D. A. Hutchins, and F. Fu. 2011. CO2 and vitamin B12 interactions determine bioactive trace metal requirements of a subarctic Pacific diatom. ISME J. **5**: 1388–1396. doi:10.1038/ismej.2010.211

Koch, F., T. K. Hattenrath-Lehmann, J. A. Goleski, S. Sañudo-Wilhelmy, N. S. Fisher, and C. J. Gobler. 2012.

Vitamin B 1 and B 12 uptake and cycling by plankton communities in coastal ecosystems. Front. Microbiol. **3**: 1–11. doi:10.3389/fmicb.2012.00363

Kromkamp, J. C., and R. M. Forster. 2003. The use of variable fluorescence measurements in aquatic ecosystems: Differences between multiple and single turnover measuring protocols and suggested terminology. Eur. J. Phycol. **38**: 103–112. doi:10.1080/0967026031000094094

Lam, P. J., J. K. B. Bishop, C. C. Henning, M. A. Marcus, G. A. Waychunas, and I. Y. Fung. 2006. Wintertime phytoplankton bloom in the subarctic Pacific supported by continental margin iron. Global Biogeochem. Cycles **20**: 1–12. doi:10.1029/2005GB002557

Lam, P. J., and J. K. B. Bishop. 2008. The continental margin is a key source of iron to the HNLC North Pacific Ocean. Geophys. Res. Lett. **35**: 1–5. doi:10.1029/2008GL033294

Langmead, B., and S. L. Salzberg. 2012. Fast gapped-read alignment with Bowtie 2. Nat. Methods **9**: 357–359. doi:10.1038/nmeth.1923

Li, H., and others. 2009. The sequence alignment/map format and SAMtools. Bioinformatics **25**: 2078–2079. doi:10.1093/bioinformatics/btp352

Li, S., and J. E. Cronan. 1993. Growth rate regulation of *Escherichia coli* acetyl coenzyme A carboxylase, which catalyzes the first committed step of lipid biosynthesis. J. Bacteriol. **175**: 332–340.

Lin S., and J. E. Cronan. 2012. The BioC O-methyltransferase catalyzes methyl esterification of malonyl-acyl carrier protein, an essential step in biotin synthesis. J. Biol. Chem. **287**: 37010–37020. doi:10.1074/jbc.M112.410290

Lohmann, A., M. A. Schottler, C. Brehelin, F. Kessler, R. Bock, E. B. Cahoon, and P. Dormann. 2006. Deficiency in phylloquinone (vitamin K1) methylation affects prenyl quinone distribution, photosystem I abundance, and anthocyanin accumulation in the Arabidopsis AtmenG mutant. J. Biol. Chem. **281**: 40461–40472. doi:10.1074/jbc.M609412200

Lommer, M., and others. 2012. Genome and low-iron response of an oceanic diatom adapted to chronic iron limitation. Genome Biol. **13**: R66. doi:10.1186/gb-2012-13-7-r66

Marchetti, A., M. T. Maldonado, E. S. Lane, and P. J. Harrison. 2006. Iron requirements of the pennate diatom Pseudo-nitzschia: Comparison of oceanic (high-nitrate, low-chlorophyll waters) and coastal species. Limnol. Oceanogr. **51**: 2092–2101. doi:10.4319/lo.2006.51.5.2092

Marchetti, A., and P. J. Harrison. 2007. Coupled changes in the cell morphology and elemental (C, N, and Si) composition of the pennate diatom Pseudo-nitzschia due to iron deficiency. Limnol. Oceanogr. **52**: 2270–2284. doi:10.4319/lo.2007.52.5.2270

Marchetti, A., and others. 2009. Ferritin is used for iron storage in bloom-forming marine pennate diatoms. Nature **457**: 467–470. doi:10.1038/nature07539

Marchetti, A., and others. 2012. Comparative metatranscriptomics identi fi es molecular bases for the physiological responses of phytoplankton to varying iron availability. Proc. Natl. Acad. Sci. **109**: E317–E325. doi:10.1073/pnas.1118408109

Marchetti, A., D. Catlett, B. M. Hopkinson, K. Ellis, and N. Cassar. 2015. Marine diatom proteorhodopsins and their potential role in coping with low iron availability. ISME J. **9**: 2745–2748. doi:10.1038/ismej.2015.74

Moore, J. K., S. C. Doney, D. M. Glover, and I. Y. Fung. 2002. Iron cycling and nutrient-limitation patterns in surface waters of the World Ocean. Deep-Sea Res. II **49**: 463–507. doi:10.1016/S0967-0645(01)00109-6

Morrissey, J., and others. 2015. A novel protein, ubiquitous in marine phytoplankton, concentrates iron at the cell surface and facilitates uptake. Curr. Biol. **25**: 364–371. doi:10.1016/j.cub.2014.12.004

Muralla, R., E. Chen, C. Sweeney, J. A. Gray, A. Dickerman, B. J. Nikolau, and D. Meinke. 2008. A bifunctional locus (BIO3-BIO1) required for biotin biosynthesis in Arabidopsis. Plant Physiol. **146**: 60–73. doi:10.1104/pp.107.107409

Nelson, D. M., D. J. DeMaster, R. B. Dunbar, and W. O. Smith. 1996. Cycling of organic carbon and biogenic silica in the Southern Ocean: Estimates of water-column and sedimentary fluxes on the Ross Sea continental shelf. J. Geophys. Res. **101**: 18519. doi:10.1029/96JC01573

Noble, R. T., and J. A. Fuhrman. 1998. Use of SYBR Green I for rapid epifluorescence counts of marine viruses and bacteria. Aquat. Microb. Ecol. **18**: 114–118. doi:10.3354/ame014113

Pejchal, R., and M. L. Ludwig. 2005. Cobalamin-independent methionine synthase (MetE): A face-to-face double barrel that evolved by gene duplication. PLoS Biol. **3**: e31. doi:10.1371/journal.pbio.0030031

Pfaffen, S., J. M. Bradley, R. Abdulqadir, M. R. Firme, G. R. Moore, N. E. Le Brun, and M. E. P. Murphy. 2015. A diatom ferritin optimized for iron oxidation but not iron storage. J. Biol. Chem. **290**: 28416–28427. doi:10.1074/jbc.M115.669713

Price, N. M., G. I. Harrison, J. G. Hering, R. J. Hudson, P. M. V. Nirel, B. Palenik, and F. M. M. Morel. 1989. Preparation and chemistry of the artificial algal culture medium Aquil. Biol. Oceanogr. **6**: 443–461. doi:10.1080/01965581.1988.10749544

Provasoli, L. 1963. Organic regulation of phytoplankton fertility, pp. 165–219. In M. N. Hill, (Ed.), The composition of seawater: Comparative and descriptive oceanography. The sea: ideas and observations on progress in the study of the seas, volume 2. Wiley Interscience: New York.

Robertson, G., and others. 2010. De novo assembly and analysis of RNA-seq data. Nat. Methods **7**: 909–912. doi:10.1038/nmeth.1517

Robinson, M. D., and G. K. Smyth. 2008. Small-sample estimation of negative binomial dispersion, with applications to SAGE data. Biostatistics **9**: 321–332. doi:10.1093/biostatistics/kxm030

Robinson, M. D., D. J. McCarthy, and G. K. Smyth. 2010. edgeR: A Bioconductor package for differential expression

analysis of digital gene expression data. Bioinformatics **26**: 139–140. doi:10.1093/bioinformatics/btp616

Rodionov, D. A., A. G. Vitreschak, A. A. Mironov, and M. S. Gelfand. 2003. Comparative Genomics of the Vitamin B12 Metabolism and Regulation in Prokaryotes. J. Biol. Chem. **278**: 41148–41159. doi:10.1074/jbc.M305837200

Saito, M. A., A. E. Noble, A. Tagliabue, T. J. Goepfert, C. H. Lamborg, and W. J. Jenkins. 2013. Slow-spreading submarine ridges in the South Atlantic as a significant oceanic iron source. Nat. Geosci. **6**: 775–779. doi:10.1038/ngeo1893

Sanudo-Wilhelmy, S. A., C. J. Gobler, M. Okbamichael, G. T. Taylor, V. Analysis, and B. S. Cove. 2006. Regulation of phytoplankton dynamics by vitamin B 12. Geophys. Res. Lett. **33**: 10–13. doi:10.1029/2005GL025046

Sañudo-Wilhelmy, S. A., and others. 2012. Multiple B-vitamin depletion in large areas of the coastal ocean. Proc. Natl. Acad. Sci. USA. **109**: 14041–14045. doi:10.1073/pnas.1208755109

Sanudo-Wilhelmy, S. A., G. Laura, C. Suffridge, and E. A. Webb. 2014. The role of B vitamins in marine biogeochemistry. Annu. Rev. Mar. Sci. **6**: 339–367. doi:10.1146/annurev-marine-120710-100912

Schuback, N., C. Schallenberg, C. Duckham, M. T. Maldonado, and P. D. Tortell. 2015. Interacting effects of light and iron availability on the coupling of photosynthetic electron transport and CO_2-assimilation in marine phytoplankton. PLoS One **10**: e0133235. doi:10.1371/journal.pone.0133235

Shakoury-Elizeh, M., and others. 2004. Transcriptional remodeling in response to iron deprivation in *Saccharomyces cerevisiae*. Mol. Biol. Cell **15**: 1233–1243. doi:10.1091/mbc.E03-09-0642

Smetacek, V., and others. 2012. Deep carbon export from a Southern Ocean iron-fertilized diatom bloom. Nature **487**: 313–319. doi:10.1038/nature11229

Stein, A. F., R. R. Draxler, G. D. Rolph, B. J. B. Stunder, M. D. Cohen, and F. Ngan. 2015. NOAA's HYSPLIT atmospheric transport and dispersion modeling system. Bull. Am. Meteorol. Soc. **96**: 2059–2077. doi:10.1175/BAMS-D-14-00110.1

Streit, W. R., and P. Entcheva. 2003. Biotin in microbes, the genes involved in its biosynthesis, its biochemical role and perspectives for biotechnological production. Appl. Microbiol. Biotechnol. **61**: 21–31. doi:10.1007/s00253-002-1186-2

Strzepek, R. F., K. A. Hunter, R. D. Frew, P. J. Harrison, and P. W. Boyd. 2012. Iron – light interactions differ in Southern Ocean phytoplankton. Limnol. Oceanogr. **57**: 1182–1200. doi:10.4319/lo.2012.57.4.1182

Tang, Y. Z., F. Koch, and C. J. Gobler. 2010. Most harmful algal bloom species are vitamin B 1 and B 12 auxotrophs. Proc. Natl. Acad. Sci. USA. **107**: 20756–20761. doi:10.1073/pnas.1009566107

Warren, M. J., E. Raux, H. L. Schubert, and J. C. Escalante-Semerena. 2002. The biosynthesis of adenosylcobalamin (vitamin B_{12}). Nat. Prod. Rep. **19**: 390–412. doi:10.1039/b108967f

Webb, M. E., A. Marquet, R. R. Mendel, F. Rebeille, and A. G. Smith. 2007. Elucidating biosynthetic pathways for vitamins and cofactors. Nat. Prod. Rep. **24**: 988–1008. doi:10.1039/b703105j

Zhang, H., Y. Zhuang, J. Gill, and S. Lin. 2013. Proof that dinoflagellate spliced leader (DinoSL) is a useful hook for fishing dinoflagellate transcripts from mixed microbial samples: Symbiodinium kawagutii as a case study. Protist **164**: 510–527. doi:10.1016/j.protis.2013.04.002

Zöllner, E., H.-G. Hoppe, U. Sommer, and K. Jürgens. 2009. Effect of zooplankton-mediated trophic cascades on marine microbial food web components (bacteria, nanoflagellates, ciliates). Limnol. Oceanogr. **54**: 262–275. doi:10.4319/lo.2009.54.1.0262

Acknowledgments

We are grateful to M. Robert (IOS) and other scientists from the Institute of Ocean Sciences as well as the crew of the CCGS J.P. Tully for their support at sea during the 2013-17 Line-P cruise. We thank C. Suffridge (USC) for seawater B-vitamin preconcentration method training, S. Loftus (DUML) for guidance with flow cytometry and J. Benjamin (UNC) for assistance with chlorophyll extractions. J. Cullen (UVic) provided the NOAA HYSPLIT ash trajectories of the Mt. Pavlof ash cloud. J. Roach (UNC), S. Haines (UNC), W. Gong (UNC) and D. Schruth contributed bioinformatic support. E. Bertrand (DAL) provided the JGI gene identification numbers corresponding to *CBA1* in diatoms. We are thankful for the careful review, advice, and suggestions offered by two anonymous reviewers. All RNA-Seq data was processed using UNC's Research Computing clusters. This study was supported by a National Science Foundation Grant OCE1334935 to A. M.

Conflict of Interest

None declared.

Submitted 19 July 2016
Revised 16 December 2016; 08 February 2017
Accepted 22 February 2017

Associate editor: Heidi Sosik